A numerical study of a fast axial flow CO_2 laser using Plasimo

M.W.T.M van Dort
Eindhoven University of Technology

August 2017

Supervisors: dr. ir. Jan van Dijk
              dr. ir. Diana Mihailova
              dr. ir. Wouter Graef

Abstract

The CO_2 laser has many applications, ranging from cutting or welding to usage in surgical procedures. It is therefore useful to understand its behaviour.

The gas mixture of a typical CO2 laser consists of about 77% He, 20% N_2 and only 3% CO_2. Population inversion is attained by creating a plasma, by which the species will be excited. The nitrogen is most susceptible to excitation. Collisions between excited nitrogen and CO_2 in the ground state will excite the CO_2 to the first asymmetric stretch mode, which is the upper laser level. The helium helps depopulate the first CO_2 symmetric stretch mode, which is the lower laser level. This depopulation is also reached by decay of the symmetric stretch mode to a bending mode.

The output of a CO_2 laser can be described approximately by the so-called five temperature model. This model describes six energy reservoirs, representing the total rotational and translational energy of the molecules, the energy in the vibrationally excited states of the molecules and the photon energy density. Energy transfer between the reservoirs is modelled by several processes, such as collisions between molecules and electrons or other molecules, spontaneous and stimulated emission of photons, etc.

The five temperature model was implemented in PLASIMO to calculate the solution numerically, and results were compared to an existing implementation in MATLAB as well as literature. It was found that the PLASIMO model agrees very well with both. The behaviour of the system was investigated for various input parameters, amongst others pressure, temperature and input power. The PLASIMO model proved to be faster and more robust.

Contents

Chapter 1

Introduction

The CO_2 laser is a very versatile piece of equipment. The wavelength it produces is approximately 10 μm (infrared), and its continuous wave output power can range from milliwatts up to several tens of kilowatts. There are thus many applications, ranging from e.g. medical, like laser surgery, to industrial applications like welding thick steel plates. This project was done in cooperation with ASML, who use a CO_2 laser in their extreme ultraviolet light source.

A CO_2 laser uses a gas mixture of about 77% He, 20% N_2 and only 3% CO_2. The laser transition occurs between vibrational states of CO_2: the upper laser level is the first excited level of the asymmetric stretch mode, and the lower laser level is the first excited level of the symmetric stretch mode. Population inversion is created using a plasma. The nitrogen is very susceptible for excitation to its vibrational states. Through collisions, N_2 can transfer its vibrational energy to CO_2, thus filling the upper laser level, in a process called a V-V transition. The lower laser level is depopulated through collisions with i.a. helium, in which its vibrational energy is turned to kinetic energy, a so called V-T transition.

The five temperature model uses six energy reservoirs to model the kinetic energy of the gas mixture, the total vibrational energy of each mode of both CO_2 and N_2, and the photon energy density. Several processes in which energy is transfered between these reservoirs are included, such as V-V and V-T transitions, pumping by the plasma, cooling, and of course the laser transition. This model provides further insight in the operation of a CO_2 laser, and can help in choosing operating parameters like input power, pressure, etc., to achieve the desired laser output.

Although an implementation of the five temperature model in MATLAB exists, it proved to be unreliable. For certain parameters, the simulation would take very long to complete, if a solution was found at all. Therefore, a new implementation was made in PLASIMO.

In this report, we will first treat some basic theory of lasers in general, and explain some of the processes involved in a CO_2 laser specifically. The five temperature model is described, by first explaining the six reservoirs, and next the processes that transfer energy between them.

The results of the implementation in PLASIMO were verified using the MATLAB model, and validated by comparing results to literature and by simulating some real world scenarios.

Chapter 2

Theory

2.1 Laser physics

In this section we will first introduce the basic principles of lasers: stimulated emission and population inversion. We will discuss how population inversion can be created by a method called pumping. An excellent resource about this subject is [1].

2.1.1 Basic principles

An atom or molecule can assume multiple states with various energies, such as electronically or vibrationally excited states. An excited particle can spontaneously decay to a state with lower energy in a process called radiative decay. The leftover energy is then converted to light; in other words, a photon with exactly the energy of the transition is emitted in a random direction. This is called *spontaneous emission* (see figure 2.1). The exact opposite of this process can also occur: a particle in the lower level (state 1) can be excited to the higher level (state 2) by *absorption* of a photon of exactly the right energy: $E = E_2 - E_1 = h\nu$, where h is Planck's constant and ν is the frequency of the photon.

In a medium under normal conditions, be it a solid, liquid or gas, the distribution of particles over their levels is described by the Boltzmann-distribution:

$$\frac{N_2}{g_2} = \frac{N_1}{g_1} \exp\left(-\frac{E_2 - E_1}{k_B T}\right). \tag{2.1.1.1}$$

Here N_i denotes the number of particles in a certain state, which is also known as the *population* of that level, and g_i is their degeneracy. The temperature is T, and k_B is Boltzmann's constant.

As a result of this distribution, the amount of particles in the lower level will always be higher than the amount in the upper level.

An interesting phenomenon occurs when a photon of energy $E = E_2 - E_1$ is absorbed by a particle in state 2. In that case, the particle is deexcited to the state 1, releasing another photon that is coherent with the incident photon. This means it is of exactly the same wavelength, it moves in the same direction and it's phase is equal to that of the incoming photon. This is called

stimulated emission, and it is the process the name 'laser' is based on: Light Amplification by Stimulated Emission of Radiation.

When a beam of light is sent through the gas in thermal equilibrium, absorption, emission and stimulated emission will occur. Since there are many particles in the lower energy state, it is likely that an incoming photon is absorbed. It is less likely for a photon to cause stimulated emission, since the population of the upper level is lower. The absorbed photons are mostly emitted through radiative decay, in a random direction. Therefore, the intensity of the beam will be lower after passing through the medium.

If by some method we can change the populations of these levels in such way that an incoming photon is more likely to cause stimulated emission than it is to cause absorption, something interesting happens: the intensity of the light will increase as it passes through the gas. This state is called *population inversion*; a medium in which population inversion is attained is called an *active medium*. Generally, the levels of a system will be degenerate, meaning there are multiple states with the same energy. For population inversion to occur, the condition

$$\frac{N_2}{g_2} > \frac{N_1}{g_1} \tag{2.1.1.2}$$

must be satisfied.
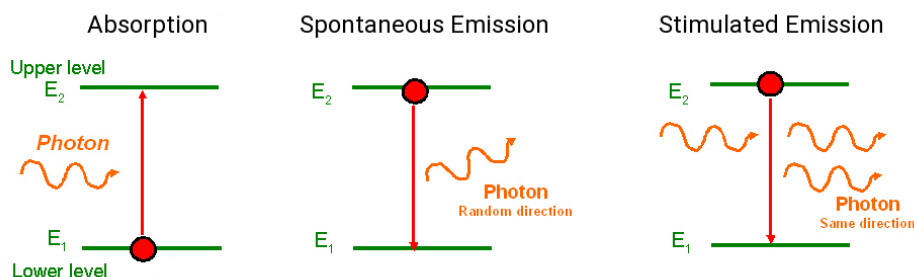
Figure 2.1: A schematic representation of absorption, spontaneous emission and stimulated emission. Image adapted from `http://www.optique-ingenieur.org/en/courses/OPI_ang_M01_C01/co/Contenu_05.html`

2.1.2 Pumping

To amplify light, we need to create population inversion. This means we need some method to increase the population of the upper laser level, without increasing that of the lower laser level. This is called *pumping*.

Figure 2.2 shows two possible methods. In the first case, (a), a three-level laser, pumping occurs between the ground level and the third level. Through some process, it quickly decays to level 2, the upper laser level. Because the ground level, which is the lower laser level, is being depleted, and the upper level is being filled, population inversion can be obtained. Note that once the lasing starts, the upper level will quickly be depopulated, and the lower level is quickly filled up again. In many cases the pumping cannot keep up with these processes, therefore schemes like this one are typical for pulse lasers.
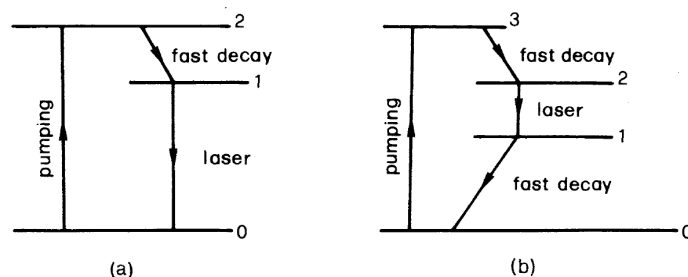
Figure 2.2: Examples of a three-level (a) and a four-level (b) pumping scheme. [1, adapted from fig 1.4]

The second case, (b), displays a four-level system. Pumping occurs from the ground state to level 3, which in turn rapidly decays to the upper laser level. Since the population of the lower laser level is naturally much less populated than the ground state, population inversion occurs much more quickly. However, to maintain population inversion, it is necessary for level 1 to be quickly depopulated. This scheme is typical for continuous wave lasers.

There are many methods to pump a medium, such as using incident light of the right frequency, creating a gas discharge, certain chemical reactions or even nuclear fission.

Once we have an active medium, we still need a photon to start the chain reaction. This photon could come from some external source. It could also come from the medium itself, since it emits photons through spontaneous emission. A photon that is emitted in the right direction could stimulate the emission of other photons. By placing mirrors on either side of the medium, we can create feedback: as the light reflects back and forth through the active medium, more and more photons are created. Power can be extracted from the laser by using a mirror that is only partially reflective. The reflectivity of the mirror must be chosen such that there is positive feedback. Some lasers have such high gain that a second mirror is unnecessary.

At some point an equilibrium will be reached, where the losses through the partially reflective mirror and other internal processes are equal to the energy gained within the active medium. Note that since a standing wave will form between the mirrors, the distance between them must be a multiple of the half wavelength.

2.1.3 Derivation using the Einstein thermodynamic approach

Knowing the populations of the upper and lower laser level, we can calculate how much a beam of incoming light is amplified.

Consider the change in a two level system due to an energy density with spectral distribution ρ_ν. The probabilities of spontaneous and stimulated transitions are given by [1, ch. 2.4.4]:

$$W_{21}^{\mathrm{sp}} = A_{21}, \tag{2.1.3.1}$$
$$W_{21}^{\mathrm{st}} = B_{21}\rho_\nu, \tag{2.1.3.2}$$
$$W_{12}^{\mathrm{st}} = B_{12}\rho_\nu, \tag{2.1.3.3}$$

where W_i is the probability and A_{21}, B_{21} and B_{12} are the Einstein coefficients for the respective processes. Note that $\tau_{\mathrm{sp}} = \frac{1}{A_{21}}$ is the relaxation time for spontaneous emission from state 2 to 1.

When considering only the influence of ρ_ν, the system must be in thermodynamic equilibrium. Then, the number of transitions from level 1 to 2 and vice versa must be equal. We thus find:

$$A_{21}N_{\mathrm{up}} + B_{21}\rho_\nu N_{\mathrm{up}} = B_{12}\rho_\nu N_{\mathrm{lo}}, \tag{2.1.3.4}$$

where N_{lo} and N_{up} are the population densities of the lower and upper laser level respectively.

According to Boltzmann, we can find the number of atoms in a state i by using:

$$\frac{N_i}{N} = \frac{g_i}{Z} \exp\left(-\frac{E_i}{kT}\right), \tag{2.1.3.5}$$

with Z the partition sum of all states, $N = \sum_i N_i$ the total particle density and E_i the energy of state i. Substituting this in 2.1.3.4, rearranging the terms and using $E_2 - E_1 = h\nu$ we find:

$$A_{21}N_{\mathrm{up}}g_2 + B_{21}N_{\mathrm{up}}g_2\rho_\nu = B_{12}N_{\mathrm{lo}}g_1 \exp\left(\frac{h\nu}{kT}\right)\rho_\nu \tag{2.1.3.6}$$

From Planck's law we know

$$\rho_\nu = N_\nu\langle E\rangle = \frac{8\pi\nu^2}{c^3}\left[\frac{h\nu}{\exp\left(\frac{h\nu}{kT}\right) - 1}\right], \tag{2.1.3.7}$$

where $N_\nu = \frac{8\pi\nu^2}{c^3}$ is the number of modes in a black body radiator at thermal equilibrium, and $\langle E\rangle$ is the mean energy of a single oscillator.

Combining 2.1.3.6 and 2.1.3.7, and rearranging terms, we then find:

$$A_{21}N_{\mathrm{up}}g_2\left[\exp\left(\frac{h\nu}{kT}\right) - 1\right] + B_{21}N_{\mathrm{up}}g_2 N_\nu h\nu = B_{12}N_{\mathrm{lo}}g_1 \exp\left(\frac{h\nu}{kT}\right) N_\nu h\nu. \tag{2.1.3.8}$$

Since this relation must be true for all T, we find:

$$B_{21}g_2 = B_{12}g_1, \tag{2.1.3.9}$$
$$\frac{A_{21}}{B_{21}} = N_\nu h\nu = \frac{8\pi h\nu^3}{c^3}. \tag{2.1.3.10}$$

The change in energy density is given by

$$
\begin{aligned}
\frac{\partial \rho_\nu}{\partial t} &= h\nu \left(W_{21}^{\mathrm{sp}} + W_{21}^{\mathrm{st}} \right) N_{\mathrm{up}} - h\nu W_{12}^{\mathrm{st}} N_{\mathrm{lo}} \\
&= h\nu A_{21} N_{\mathrm{up}} + h\nu B_{21}\rho_\nu N_{\mathrm{up}} g(\nu - \nu_0) - h\nu B_{12}\rho_\nu N_{\mathrm{lo}} g(\nu - \nu_0) \\
&= h\nu A_{21} N_{\mathrm{up}} + h\nu \rho_\nu B_{21} \left(N_{\mathrm{up}} - \frac{B_{12}}{B_{21}} N_{\mathrm{lo}} \right) g(\nu - \nu_0)
\end{aligned}
\tag{2.1.3.11}
$$

Using the relations 2.1.3.9 and 2.1.3.10 we find:

$$
\begin{aligned}
\frac{\partial \rho_\nu}{\partial t} &= h\nu A_{21} N_{\mathrm{up}} + h\nu \rho_\nu B_{21} \left(N_{\mathrm{up}} - \frac{g_2}{g_1} N_{\mathrm{lo}} \right) g(\nu - \nu_0) \tag{2.1.3.12} \\
&= h\nu A_{21} N_{\mathrm{up}} + h\nu \rho_\nu A_{21} \frac{c^3}{8\pi h\nu^3} \left(N_{\mathrm{up}} - \frac{g_2}{g_1} N_{\mathrm{lo}} \right) g(\nu - \nu_0) \tag{2.1.3.13}
\end{aligned}
$$

Because of the linewidth of the spectral density ρ_ν we introduced a factor $g(\nu - \nu_0)$, with $\int g(\nu - \nu_0)\mathrm{d}\nu = 1$.

For clarity, we define:

$$
\begin{aligned}
W &= A_{21} \frac{c^3}{8\pi h\nu^3} g(\nu - \nu_0), \tag{2.1.3.14} \\
\Delta N &= \left(N_{\mathrm{up}} - \frac{g_2}{g_1} N_{\mathrm{lo}} \right). \tag{2.1.3.15}
\end{aligned}
$$

Also, recall that $A_{21} = \tau_{\mathrm{sp}}^{-1}$, which leaves us with:

$$
\frac{\partial \rho_\nu}{\partial t} = h\nu \left[\frac{N_{\mathrm{up}}}{\tau_{\mathrm{sp}}} + W\Delta N \right]
\tag{2.1.3.16}
$$

2.2 The CO_2 laser

A CO_2 laser uses a gas mixture containing approximately 77% nitrogen, 20% helium and only 3% carbon dioxide. Pumping of the upper laser level is done by creating a plasma.

In this section we will explain the choice of gas mixture, and the processes involved in the operation of the laser. To this end, will first describe the excited states of CO_2 and their respective energy levels. Then we will take a look at the reactions that take place in the plasma.

2.2.1 CO_2 degrees of freedom

As any free particle, a CO_2 molecule has three translational degrees of freedom. Opposed to a mono-atomic gas, molecules can also rotate. Since carbon dioxide is a linear molecule, meaning it has an axis of symmetry, there are only two possible rotational modes.

CO_2 is a molecule consisting of three atoms, which has three vibrational modes [2, ch. 2]. The simplest is the so called symmetric stretch mode. In this mode, both oxygen atoms vibrate out of phase, in the axial direction. In the asymmetric stretch mode the oxygen atoms vibrate in phase in the axial direction. Lastly, there is a bending mode, where the carbon vibrates perpendicular to the linear axis. Figure 2.3 shows the degrees of freedom of CO_2, including the rotational and vibrational modes. Note that since the bending breaks the symmetry of the molecule, two coordinates are necessary to describe the motion. Therefore, the bending modes are doubly degenerate.

From quantum mechanics follows that the energy at which the molecule can vibrate is quantized. Each vibrational mode thus has several distinct levels. This is shown in figure 3.1. The rotational energy is also quantized. Because the energy difference between rotational levels is much smaller than between vibrational levels, we consider it as each vibrational level having many rotational sublevels.

To indicate the vibrational state of a molecule, the following notations are used: $CO_2(n_i, n_j, n_k; m)$ indicates a CO_2 molecule that is excited to level n_i in the symmetric stretch mode, level n_j in the bending mode and level n_k in the asymmetric stretch mode. The rotational excitation is indicated by quantum number m. In reactions where the rotational level is irrelevant, this number may be omitted. For example, $CO_2(0, 0, 0; 0)$ is in the ground state, whereas $CO_2(0, 0, 1)$ is excited to the first level in the asymmetric stretch mode.

Nitrogen, being a diatomic molecule also has a symmetric stretch mode. Similarly to CO_2, we can indicate e.g. the first excited stretch mode of N_2 as $N_2(1)$. We will use these definitions later.
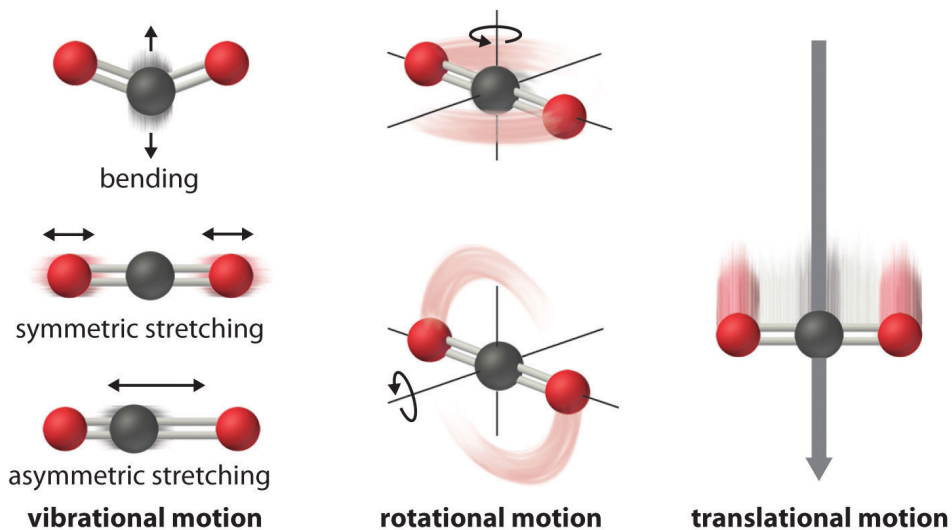
Figure 2.3: The degrees of freedom of a CO_2 molecule. Image from: `https://chem.libretexts.org/Textbook_Maps/General_Chemistry_Textbook_Maps/Map%3A_Chemistry_(Averill_and_Eldredge)/Chemical_Thermochemistry/18.4_Entropy_Changes_and_the_Third_Law_of_Thermodynamics`
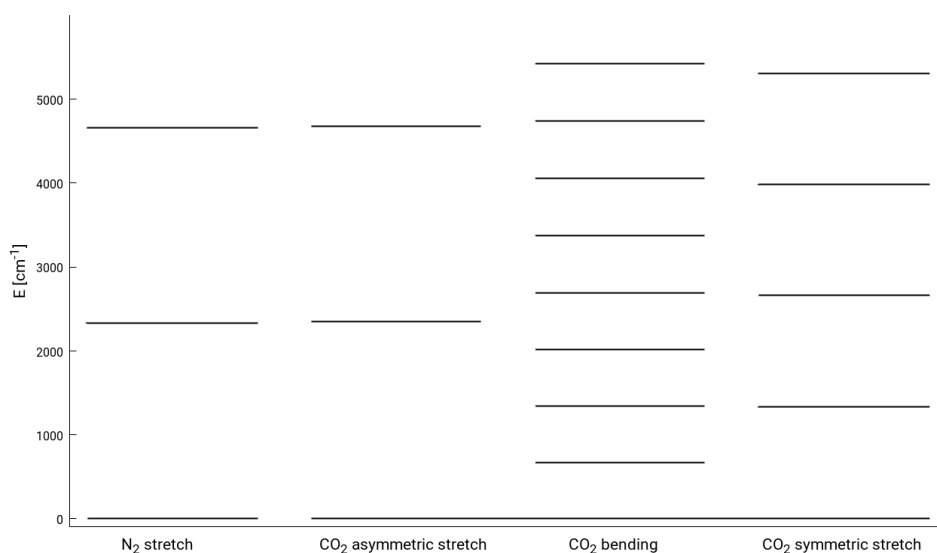
Figure 2.4: The energy of some of the vibrationally excited states of CO_2 and N_2.

2.2.2 Laser levels of CO_2

In a CO_2 laser, the upper laser level is the 19th rotational level of the first asymmetric stretch mode: $CO_2(0, 0, 1; 19)$. The lower laser level is the 20th rotational level of the first symmetric stretch mode: $CO_2(1, 0, 0; 20)$. The wavelength of the light emitted in this transition is 10.59 µm, far infrared. See figure 2.5.

2.2.3 Processes in a CO_2 laser

This section describes the processes that take place in the laser, which cause molecules to switch from one vibrational state to another.

2.2.3.1 Pumping

The laser operates at 300 K[a], at which $k_B T \approx 210\,\mathrm{cm}^{-1}$. This is low compared to the energy of the first levels of each vibrational mode. Therefore almost all CO_2 molecules will be in their (vibrational) ground state.

To excite the molecules we create a plasma. The gas is contained in a tube, at either end of which an electrode is placed. By applying a sufficiently large voltage we can create a plasma. The free electrons in the plasma are accelerated by the electric field. When they collide with a molecule, their kinetic energy can be absorbed by the molecule as it is excited vibrationally.

The collisional cross section for these reactions is found by solving the Electron Energy Distribution Function, or EEDF. This is a challenging problem on its own [3], and in this report we will not go into detail. For CO_2, these cross sections are very small, making this a very inefficient way of pumping.

The collisional cross section for N_2 is much larger, meaning it can be excited much more easily by electrons. For this, and other reasons we will see in section 2.2.3.2, we add nitrogen to our gas mixture.

2.2.3.2 V-V interactions

A V-V interaction (Vibrational - Vibrational), is an interaction where vibrational energy is transfered from one molecule to another through a collision. In this process, the second molecule is excited vibrationally. There are several of these interactions that play an important role in the operation of the laser.

As we can see in figure 3.1, the energy of the first excited state of N_2 (2330 cm^{-1}) is very close to that of the first asymmetric stretch mode of CO_2 (2349 cm^{-1}). This means that they can easily transfer energy through a V-V interaction. The remaining energy that is needed is much smaller than $k_B T$, and thus comes from the kinetic energy of the molecules. By pumping N_2, we can thus selectively pump the upper laser level, without pumping the lower laser level.

---

[a]This is the inlet temperature of the gas. See section 2.2.3.4.

The corresponding reaction is:

$$CO_2(0,0,0) + N_2(1) \rightarrow CO_2(0,0,1) + N_2(0). \tag{2.2.3.1}$$

Since the energy difference between excited states of N_2 is almost constant, this reaction can also occur with N_2 that is excited to a higher state. Up to the 4th excited state of N_2, $k_B T$ is still larger than the energy deficit, and the reaction can still occur [2, ch. 3.7].

The energy of the second bending mode is almost equal to that of the first symmetric stretch mode. Because of this, the lower laser level is quickly depopulated through V-V interactions between these states. In this interaction, the CO_2 molecule can collide with any other particle in the gas, indicated by M in the reaction:

$$CO_2(1,0,0) + M \rightarrow CO_2(0,2,0) + M. \tag{2.2.3.2}$$

Of course, these interactions also occur between other vibrational modes and levels of CO_2, but as the difference in energy between levels becomes larger, the reaction rates become much lower.

Note that the energy difference between levels in the same vibrational modes is almost constant (see figure 3.1). This means that molecules in the same vibrational mode can very easily transfer energy amongst each other through V-V interactions.

2.2.3.3 V-T interactions

In a V-T interaction (Vibrational - Translational), a vibrationally excited molecule collides with any other particle, and in doing so it exchanges vibrational energy to kinetic energy. These interactions are important to help depopulate the symmetric stretch mode and the bending mode. Because of the increase in kinetic energy of the gas, the temperature rises.

Helium is added to the gas mixture, because it's very effective at depopulating the lower laser level through these interactions [2, ch 3.10].

2.2.3.4 Cooling

Since the gas heats up through V-T interactions, according to Boltmann's distribution the population of the lower laser level will increase. It's even possible that the population inversion is lost. Therefore the gas mixture must be cooled. To this end, the gas is pumped around continuously, and cooled before it's pumped back into the tube.
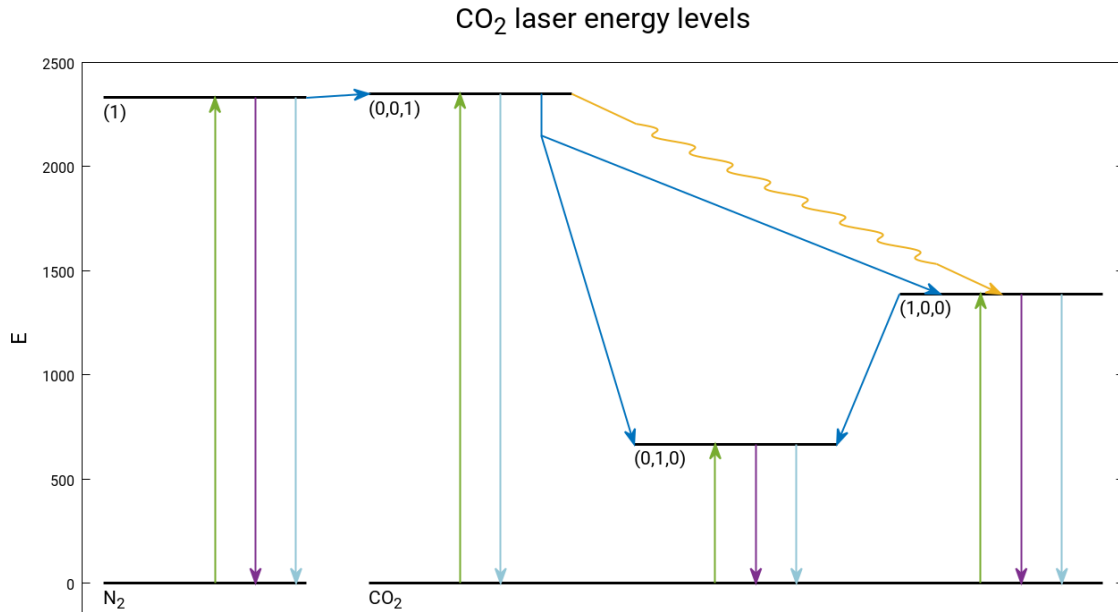
Figure 2.5: A representation of the energy levels of the excited states of N_2 and CO_2, and included processes: pumping in green, V-V interactions in dark blue, V-T interactions in purple, and cooling in light blue. The laser transition is the wavy line in yellow.

2.2.4 Practical aspects of the fast axial flow CO_2 laser

The gas mixture is contained in a glass tube. To create the plasma there are 2 electrodes, one on either side of the tube. The cathode is ring-shaped, the anode consists of 4 pins protruding straight into the tube, perpendicular to its neighbours. By applying a (sufficiently large) voltage, the plasma is created. To regulate the current, a ballast resistor of 15 kΩ is added in series to the tube. The voltage applied is 19 kV, the current is 125 mA [4, ch. 4].

Since the gas heats up as the lasing occurs, it must be cooled. To that end, cold gas is continually being pumped through the tube. Cold gas enters the tube at the anode, and leaves at the cathode. See figure 2.6. The gas is cooled using a low pressure heat exchanger, pressurized and then cooled again using a high pressure heat exchanger, to remove the heat caused by the compression.

Eight of these tubes are arranged in a square setup, with mirrors on the corners at $45°$ to guide the laser beam. In one corner there are two seperate mirrors perpendicular to the laser beam, one of which is only partially reflective. See figure 2.7.
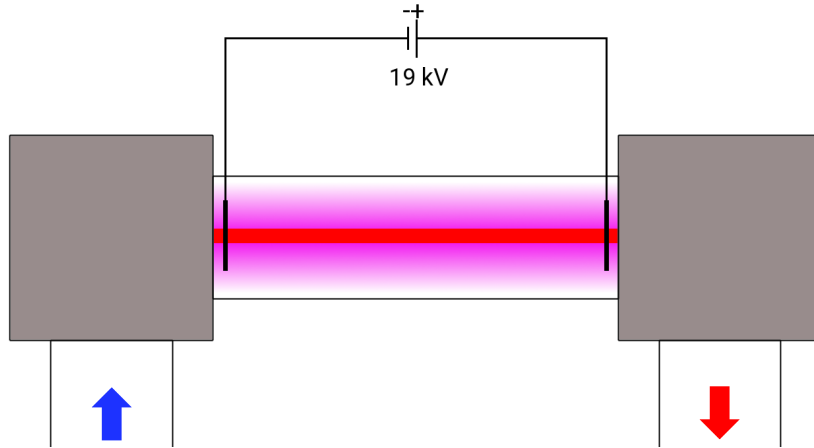
Figure 2.6: A schematic representation of a single laser tube containing plasma and the electrodes. The blue arrow indicates the inflow of cold gas, and the red arrow shows the outflow of hot gas.
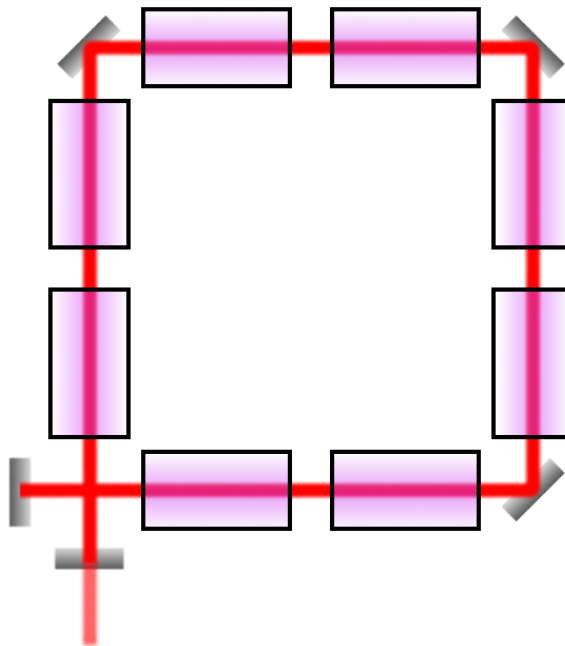
Figure 2.7: A schematic representation of the CO_2 laser, showing the eight tubes containing plasma and the mirrors. The path of the laser beam is shown in red. The partially reflective mirror can be seen at the bottom.

Chapter 3

The 5 temperature model

In this chapter we will introduce the 5 temperature model used to simulate the behaviour of the laser.

In the first part we will introduce the 6 energy reservoirs used:

- E_{TR} the kinetic (translational + rotational) energy of all particles
- E_1, all vibrational energy of CO_2 molecules in any symmetric stretch mode
- E_2, all vibrational energy of CO_2 molecules in any bending mode
- E_3, all vibrational energy of CO_2 molecules in any asymmetric stretch mode
- E_4, all vibrational energy of N_2 molecules in any stretch mode
- E_ν, the energy of all photons of frequency ν within the system

Then we will discuss the influence of the involved processes on each reservoir:

- Electrical input power
- Convective gas cooling
- Vibrational kinetics: V-V and V-T interactions
- Laser field coupling

3.1 The energy reservoirs

In thermal equilibrium, the population of each energy level is described by Boltzmann's distribution. Through the aforementioned processes this equilibrium is disturbed. This model describes the deviation from this equilibrium for each reservoir.
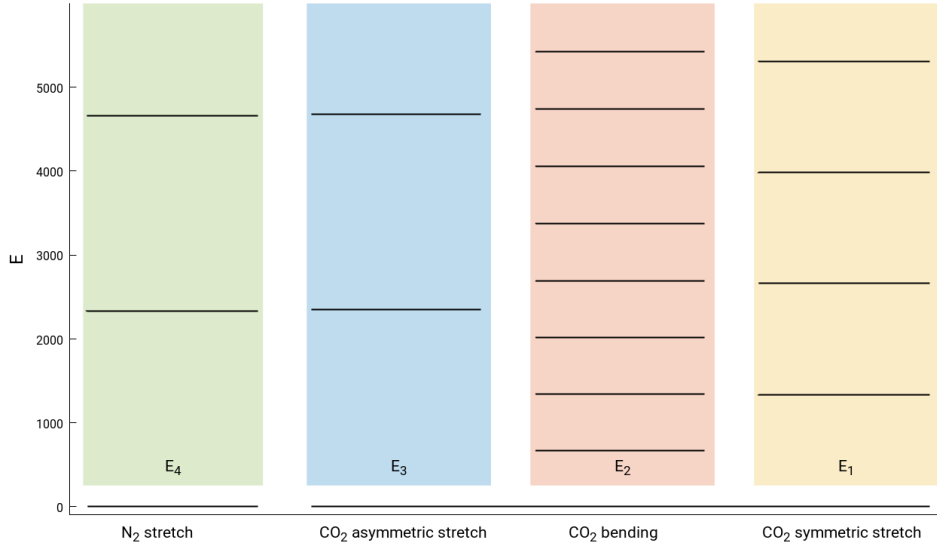
Figure 3.1: The energy of some of the vibrationally excited states of CO_2 and N_2. The colored boxes represent the energy reservoirs E_1 through E_4.

3.1.1 The translational and rotational energy E_{TR}

The kinetic energy density of the gas consists of two parts: the translational energy E_T and the rotational energy E_R. In this model the sum of these energies, $E_{TR} = E_T + E_R$, is considered to be one reservoir.

Many processes, such as collisions between molecules that cause their vibrational states to change, are exothermic. The excess energy will increase the kinetic energy of the molecules. These processes will thus cause an increase in E_{TR}. In the same way, endothermic processes can drain energy from E_{TR}.

3.1.1.1 Translational energy

The translational energy density of the gas can be calculated using the enthalpy. For simplicity, E_T is defined in such way that the energy of the cold, 'fresh' gas, is zero: $T_{ref} = T_0$, $h_{ref} = 0$. Also, the specific heat of the gas is assumed constant: $\partial c_p / \partial T \approx 0$. Applying the ideal gas law, we find [4, ch. 2.1.2.1]:

$$E_T = \frac{p c_p}{R} \ln\left(\frac{T}{T_0}\right). \tag{3.1.1.1}$$

3.1.1.2 Rotational energy

The rotational energy of a molecule in the jth excited rotational state, and the energy difference between two adjacent levels is given by [4, ch 2.1.2.2]:

$$\frac{e_{\text{R}}(j)}{hc_0} = B[j(j+1)] - D[j(j+1)]^2 + H[j(j+1)]^3 + \cdots , \qquad (3.1.1.2)$$

$$e_{\text{R}}(j+1) - e_{\text{R}}(j) \approx 2hc_0 B(j+1), \qquad (3.1.1.3)$$

$$B = \frac{h}{8\pi^2 Ic_0}, \qquad (3.1.1.4)$$

where B is the moment of inertia of the molecule, the higher order terms are negligible.

In normal circumstances, the rotational levels are populated according to the Boltzmann distribution. The laser transition occurs between specifically the 19th rotational sublevel of the upper laser level, and the 20th of the lower. Therefore, this distribution is obviously disturbed. However, the rotational relaxation time is in the order of $\tau_{\text{R}} \approx 1$ ns at typical pressures ($\sim 10^5$ Pa) [5]. Therefore, for timescales larger than τ_{R}, the difference between the rotational and translational temperature is negligible. Thus, we can describe both E_{T} and E_{R} using the same reservoir E_{TR}.

We can then describe this distribution as

$$\frac{N_j}{N_0} = g_j \exp\left(-\frac{e_{\text{R}}(j)}{kT_{\text{R}}}\right), \qquad (3.1.1.5)$$

where $g_j = 2j + 1$ is the rotational degeneration, for timescales $> \tau_{\text{R}}$. Now we can calculate the total rotational energy:

$$E_{\text{R}} = \sum_{j=0}^{\infty} N_j e_{\text{R}}(j) \qquad (3.1.1.6)$$

Since CO_2 is a linear molecule, it has 2 rotational degrees of freedom. In thermal equilibrium, where $T_{\text{R}} = T$, the rotational energy can thus be described by:

$$E_{\text{R}} = 2r\frac{k_{\text{B}}T}{2}N = rp. \qquad (3.1.1.7)$$

Here r is the number of rotational axes, with the factor 2 because of the two angles needed to describe an axis. The energy per rotational degree of freedom is $1/2k_{\text{B}}T$. From equipartition, $p = Nk_{\text{B}}T$ per unit volume, then follows $E_{\text{R}} = rp$.

3.1.2 The energy of the vibrational modes: E_1, E_2, E_3 and E_4

The description of the energy densities of the vibrationally excited states of CO_2 and N_2 are quite similar. E_1, E_2 and E_3 represent the total vibrational energy of all CO_2-molecules in the symmetric stretch modes, the bending modes and the asymmetric stretch modes, respectively. Likewise, E_4 represents the energy of N_2 in its stretch modes.

As mentioned in section 2.2.3.2, molecules in the same vibrational mode can exchange energy amongst themselves very easily. Therefore, within each mode an equilibrium is reached. We can

thus describe the population for each level within a reservoir using the Boltzmann distribution, with each reservoir having its own temperature. Hence the name: 5 temperature model.

Also, because of the constant energy difference between the levels, they can be modeled as a simple harmonic oscillator, where $E_i = h\nu_i$. Using this knowledge, we can find the energy for each level at local thermodynamic equilibrium:

$$E_1^{\text{eq}} = N_{\text{CO}_2} G_1 \left[\exp\left(\frac{G_1}{k_{\text{B}}T}\right) - 1 \right]^{-1}, \tag{3.1.2.1}$$

$$E_2^{\text{eq}} = 2 N_{\text{CO}_2} G_2 \left[\exp\left(\frac{G_2}{k_{\text{B}}T}\right) - 1 \right]^{-1}, \tag{3.1.2.2}$$

$$E_3^{\text{eq}} = N_{\text{CO}_2} G_3 \left[\exp\left(\frac{G_1}{k_{\text{B}}T_1} + \frac{G_2}{k_{\text{B}}T_2} + \frac{G_3 - G_2 - G_1}{k_{\text{B}}T}\right) - 1 \right]^{-1}, \tag{3.1.2.3}$$

$$E_4^{\text{eq}} = N_{\text{N}_2} G_4 \left[\exp\left(\frac{G_4}{k_{\text{B}}T}\right) - 1 \right]^{-1}, \tag{3.1.2.4}$$

$$\tag{3.1.2.5}$$

where $G_i = h\nu_i$, the energy of the respective levels, and the vibrational temperature

$$T_i = \frac{G_i/k_{\text{B}}}{\ln(NG_i/E_i + 1)}, \tag{3.1.2.6}$$

where $i = \{1, 2, 3, 4\}$.

The factors N_{CO_2} and N_{N_2} are the number of CO_2 and N_2 molecules in the system, respectively.

Note that E_2^{eq} is doubly degenerate: the vibration of the molecule must be described by two independent variables. The energy in that level is therefore adjusted by a factor 2.

An extensive derivation can be found in [4, ch. 2.1.2.3], [6, ch. 2] and [7].

3.1.3   The photon energy density E_ν

A CO_2 laser can emit light at various frequencies, corresponding to the modes involved in the laser transition. In this model we only account for one frequency, ν. Therefore we can easily find the energy in the radiation field by summing the energy of the photons of this frequency per unit volume:

$$E_\nu = h\nu N_\nu = \frac{I_\nu}{c_0}, \tag{3.1.3.1}$$

where I_ν [W/m^2] is the radiation intensity in the resonator, defined as the sum of a left-bound and a right-bound wave, averaged over a period of $1/\nu$ and one wavelength λ [4, ch. 2.1.2.4].

3.2   Energy transfer equations

The energy in each reservoir is affected by many processes. In this model we take into account the electrical energy that is pumped into the system, collisions between molecules in various

excited states, convective cooling of the gas and processes involved in emission and absorption of light.

Many processes involve terms of the form

$$\frac{\partial E_i}{\partial t} = -\frac{E_i - E_i^\alpha}{\tau_{i,\alpha}}. \tag{3.2.0.1}$$

Assuming $\tau_{i,\alpha}$ is constant, the solution is given by

$$E_i(t) - E_i^\alpha = B \exp\left(-\frac{t}{\tau_{i,\alpha}}\right), \tag{3.2.0.2}$$

where E_i^α is the equilibrium energy of process α, and B is a factor depending on boundary conditions. These terms will thus cause an exponential decay of the energy towards its equilibrium value; the relaxation time $\tau_{i,\alpha}$ is the time after which the difference from the equilibrium energy will have been reduced by a factor $1/e$. Note that in reality the relaxation time depends on, among others, the temperature of the reservoirs, and the decay will thus not be exactly exponential.

3.2.1 Electrical input power

The electrical current through the plasma is determined almost completely by the electron current, since the mobility of electrons is much higher than that of the other species in the plasma. We thus assume that all electrical power is absorbed by the free electrons in the plasma.

Because of collisions between electrons and molecules, molecules can gain kinetic or vibrational energy. In this way, electrical energy can be pumped into the system. The evolution of the respective energies can simply be described by:

$$\left.\frac{\partial E_i}{\partial t}\right|_{\text{in}} = \chi_i P_{\text{in}}, \tag{3.2.1.1}$$

where again $i = \{\text{TR}, 1, 2, 3, 4\}$, P_{in} is the total electrical energy put into the system, and χ_i is the fraction of the electrical energy that goes into each level, also called the pumping fractions.

In most cases, not all of the electrical energy will be absorbed by one of the reservoirs. The remainder will be used by electronic excitation of the species. Since these processes are not included in the model, they can be viewed as a loss term of the power: $\chi_{\text{el}} P_{\text{in}}$. The total power must, of course, be conserved, thus: $\sum_i \chi_i + \chi_{\text{el}} = 1$.

3.2.1.1 The pumping fractions χ_i

The distribution of the input power over the energy reservoirs is determined by the so-called Electron Energy Distribution Function, which depends on the energy of the electrons and on the collisional cross section of each species. The values for these fractions are determined by solving the Boltzmann equation numerically, in our case using the Boltzmann-solver Bolsig+ [3].

In general, the pumping fraction for excitation of N_2 will be much larger than the other fractions. In our model, the fractions are calculated once for the appropriate plasma parameters and used as such in the simulation. The fractions depend on amongst others the gas mixture and the electric field.

3.2.2 Convective gas cooling

Since there is a constant flow of gas through the tube, hot gas leaves the laser and cold gas enters it. Using $E_i^{T_0} = E_i(T_0)$ as the energy of the gas as it enters the laser, and τ_d as the residence time of the gas in the laser, we can thus describe this process as:

$$\left.\frac{\partial E_i}{\partial t}\right|_{\text{conv}} = -\frac{E_i}{\tau_{\text{d}}} + \frac{E_i^{T_0}}{\tau_{\text{d}}} = -\frac{E_i - E_i^{T_0}}{\tau_{\text{d}}}, \tag{3.2.2.1}$$

where $i = \{\text{TR}, 1, 2, 3, 4\}$ [4, ch. 2.1.3.4].

3.2.3 Vibrational kinetics

In this section we will describe the influence of V-T and V-V interactions on the energy in the reservoirs.

3.2.3.1 V-T transitions

There are three V-T transitions taken into account in the model: the decay of CO_2 molecules in the symmetric stretch mode (reaction 3.2.3.1) or the bending mode (reaction 3.2.3.2), to the ground state, and the decay of vibrationally excited N_2 molecules to the ground state (reaction 3.2.3.3). As said before, these transitions occur when an excited molecule collides with another molecule or particle, and in doing so converting its vibrational energy into kinetic energy [6, ch. 2].

This can be described by the following reactions:

$$CO_2(1, 0, 0) + M \rightarrow CO_2(0, 0, 0) + M, \tag{3.2.3.1}$$
$$CO_2(0, 1, 0) + M \rightarrow CO_2(0, 0, 0) + M, \tag{3.2.3.2}$$
$$N_2(1) + M \rightarrow N_2(0) + M, \tag{3.2.3.3}$$

where M denotes any species that the molecule collides with.

The change in energy density for both levels is described by the equations:

$$\left.\frac{\partial E_1}{\partial t}\right|_{\text{VT}} = -\frac{E_1 - E_1^{\text{eq}}(T)}{\tau_{10}}, \tag{3.2.3.4}$$

$$\left.\frac{\partial E_2}{\partial t}\right|_{\text{VT}} = -\frac{E_2 - E_2^{\text{eq}}(T)}{\tau_{20}}, \tag{3.2.3.5}$$

$$\left.\frac{\partial E_4}{\partial t}\right|_{\text{VT}} = -\frac{E_4 - E_4^{\text{eq}}(T)}{\tau_{40}}. \tag{3.2.3.6}$$

Note that E_i is the energy density of the reservoir, whereas $E_i(T)$ is the energy calculated using the equations given in section 3.1.2. The system will thus decay towards the ambient gas energy if no disturbances are present.

Since the vibrational energy is converted to kinetic energy, the energy must be added to E_{TR}:

$$\left.\frac{\partial E_{\mathrm{TR}}}{\partial t}\right|_{\mathrm{VT}} = +\frac{E_1 - E_1^{\mathrm{eq}}(T)}{\tau_{20}} + \frac{E_2 - E_2^{\mathrm{eq}}(T)}{\tau_{20}} + \frac{E_4 - E_4^{\mathrm{eq}}(T)}{\tau_{40}}. \tag{3.2.3.7}$$

The relaxation times τ_{20} and τ_{10} are given by:

$$\tau_{20} = \left(N_{\mathrm{He}}k_{20}^{\mathrm{He}} + N_{\mathrm{CO_2}}k_{20}^{\mathrm{CO_2}} + N_{\mathrm{N_2}}k_{20}^{\mathrm{N_2}}\right)^{-1}, \tag{3.2.3.8}$$

$$\tau_{10} = 4.5\tau_{20}, \tag{3.2.3.9}$$

$$k_{20}^{\mathrm{He}} = 4.6 \cdot 10^{-16} \ \exp\left(-77T^{-1/3}\right), \tag{3.2.3.10}$$

$$k_{20}^{\mathrm{CO_2}} = 9.6 \cdot 10^{-16} \ \exp\left(-77T^{-1/3}\right), \tag{3.2.3.11}$$

$$k_{20}^{\mathrm{N_2}} = 8.1 \cdot 10^{-16} \ \exp\left(-45T^{-1/3}\right). \tag{3.2.3.12}$$

where k_{20}^{spc} [s^{-1}] is the rate coefficient for reaction 3.2.3.2, for the respective species. These coefficients are based on values found by experiment [8].

The relaxation time τ_{40} is given by [9]:

$$\tau_{40} = \frac{RT}{p_0 \cdot 4 \cdot 10^2 \cdot \left(1 - \exp\left[-\frac{3354}{T}\right]\right)}. \tag{3.2.3.13}$$

3.2.3.2 V-V transitions

There are multiple V-V transitions included in the model: the pumping of CO_2 to the asymmetric stretch mode by excited N_2, deexcitation from this mode to the symmetric stretch mode or bending mode, and deexcitation of the symmetric stretch mode to the bending mode.

Excitation of the CO_2 asymmetric stretch mode occurs when excited N_2 collides with CO_2 in the ground state, as explained in section 2.2.3.2. Since the energy difference between the excited states of nitrogen is almost the same as that of the asymmetric stretch mode of CO_2, $h\nu_3 \approx h\nu_4$, this transition occurs very easily. Up to the 4th excited state of nitrogen, the difference between each level is smaller than the average kinetic energy of the gas [2, p. 65]. So even though $h\nu_3 < h\nu_4$, the reaction can still occur, using some energy from E_{TR}.

An example of a reaction would thus be:

$$CO_2(0,0,0) + N_2(1) \rightarrow CO_2(0,0,1) + N_2(0), \tag{3.2.3.14}$$

though the same reaction could occur for N_2 going from the 4th to the 3rd excited state, etc. However, since E_4 is the sum of the energy of all vibrationally excited nitrogen, all this energy comes from the same reservoir.

The resulting equations are thus:

$$\frac{\partial E_3}{\partial t}\bigg|_{4\to3} = +\frac{G_3}{G_4}\frac{E_4 - E_4(T, T_3)}{\tau_{43}}, \tag{3.2.3.15}$$

$$\frac{\partial E_4}{\partial t}\bigg|_{4\to3} = -\frac{E_4 - E_4(T, T_3)}{\tau_{43}}, \tag{3.2.3.16}$$

$$\frac{\partial E_{\mathrm{TR}}}{\partial t}\bigg|_{4\to3} = +\left(1 - \frac{G_3}{G_4}\right)\frac{E_4 - E_4(T, T_3)}{\tau_{43}}. \tag{3.2.3.17}$$

The relaxation time and rate coefficient are given by [6, pg. 50]

$$\tau_{43} = [N_{\mathrm{CO_2}} k_{43}]^{-1}, \tag{3.2.3.18}$$

$$k_{43} = \max \begin{cases} 1.71 \cdot 10^{-6} \exp\left(\frac{-175.3}{\sqrt[3]{T}}\right) \\ 6.07 \cdot 10^{-14} \exp\left(\frac{15.3}{\sqrt[3]{T}}\right) \end{cases}. \tag{3.2.3.19}$$

Deexcitation of the CO_2 asymmetric stretch mode happens through a reaction in which a collision causes a molecule to change to a superposition of the first excited bending mode and the first excited symmetric stretch mode:

$$CO_2(0, 0, 1) + M \to CO_2(1, 1, 0) + M. \tag{3.2.3.20}$$

We thus find:

$$\frac{\partial E_3}{\partial t}\bigg|_{3\to1,2} = -\frac{E_3 - E_3(T, T_1, T_2)}{\tau_3}, \tag{3.2.3.21}$$

$$\frac{\partial E_1}{\partial t}\bigg|_{3\to1,2} = +\frac{G_1}{G_3}\frac{E_3 - E_3(T, T_1, T_2)}{\tau_3}, \tag{3.2.3.22}$$

$$\frac{\partial E_2}{\partial t}\bigg|_{3\to1,2} = +\frac{G_2}{G_3}\frac{E_3 - E_3(T, T_1, T_2)}{\tau_3}, \tag{3.2.3.23}$$

$$\frac{\partial E_{\mathrm{TR}}}{\partial t}\bigg|_{3\to1,2} = +\left(1 - \frac{G_1}{G_3} - \frac{G_2}{G_3}\right)\frac{E_3 - E_3(T, T_1, T_2)}{\tau_3}. \tag{3.2.3.24}$$

The relaxation time τ_3 is given by the following equation, with rate coefficients determined by

experiment [8]:

$$
\tau_3 = \left(N_{\text{He}} k_3^{\text{He}} + N_{\text{CO}_2} k_3^{\text{CO}_2} + N_{\text{N}_2} k_3^{\text{N}_2} \right)^{-1}
$$

$$
\times \left(\frac{\exp\left[G_1/k_{\text{B}}T_1\right] - 1}{\exp\left[G_1/k_{\text{B}}T\right] - 1} \right)
$$

$$
\times \left(\frac{\exp\left[G_2/k_{\text{B}}T_2\right] - 1}{\exp\left[G_2/k_{\text{B}}T\right] - 1} \right)
$$

$$
\times \left(\frac{\exp\left[G_3/k_{\text{B}}T\right] - 1}{\exp\left[G_1/(k_{\text{B}}T_1) + G_2/(k_{\text{B}}T_2) + (G_3 - (G_2 + G_1))/(k_{\text{B}}T)\right] - 1} \right), \tag{3.2.3.25}
$$

$$
k_3^{\text{He}} = 9.6 \cdot 10^{17} \; T^{-5.89} F(T), \tag{3.2.3.26}
$$

$$
k_3^{\text{CO}_2} = 6.87 \cdot 10^{17} \; T^{-5.89} F(T), \tag{3.2.3.27}
$$

$$
k_3^{\text{N}_2} = 2.43 \cdot 10^{17} \; T^{-5.89} F(T), \tag{3.2.3.28}
$$

$$
F(T) = \exp\left[-4223/T - 672.7 T^{-1/3} + 2683 T^{-2/3} \right]. \tag{3.2.3.29}
$$

Deexcitation of the CO_2 symmetric stretch mode to the bending mode is described by the following reaction:

$$
CO_2(1,0,0) + M \rightarrow CO_2(0,2,0) + M. \tag{3.2.3.30}
$$

This gives the following equations:

$$
\left. \frac{\partial E_1}{\partial t} \right|_{1 \to 2} = -\frac{E_1 - E_1(T_2)}{\tau_{12}}, \tag{3.2.3.31}
$$

$$
\left. \frac{\partial E_2}{\partial t} \right|_{1 \to 2} = +\frac{E_1 - E_1(T_2)}{\tau_{12}}, \tag{3.2.3.32}
$$

with the relaxation time given by [8]:

$$
\tau_{12} = \frac{1}{2} \left(N_{\text{He}} k_{12}^{\text{He}} + N_{\text{CO}_2} k_{12}^{\text{CO}_2} + N_{\text{N}_2} k_{12}^{\text{N}_2} \right)^{-1}
$$

$$
\times \left(\frac{1 - \exp[-G_2/k_{\text{B}}T_2]}{1 + \exp[-G_2/k_{\text{B}}T_2]} \right)
$$

$$
\times \left(\frac{1 + \exp[-G_2/k_{\text{B}}T]}{1 - \exp[-G_2/k_{\text{B}}T]} \right), \tag{3.2.3.33}
$$

$$
k_{12}^{\text{He}} = 4.23 \cdot 10^{-23} \; T^{3/2},
$$

$$
k_{12}^{\text{CO}_2} = 8.65 \cdot 10^{-21} \; T^{3/2}, \tag{3.2.3.34}
$$

$$
k_{12}^{\text{N}_2} = 3.68 \cdot 10^{-22} \; T^{3/2}. \tag{3.2.3.35}
$$

3.2.4 Laser field coupling

Although there are multiple frequencies at which light can be emitted and even amplified by a CO_2 laser, in this model we only consider the light with a wavelength of $\nu = 10.6\mu$m. The processes included are spontaneous and stimulated emission by CO_2 in the asymmetric stretch mode, and absorption of light by CO_2 in the symmetric stretch mode.

The laser transition occurs when a CO_2-molecule in the first excited asymmetric stretch mode and the 19$^{\text{th}}$ rotational excited state is struck by a photon of frequency ν. The molecule will then emit another photon of frequency ν, and in doing so transfer to the first excited state of the symmetric stretch mode and the 20$^{\text{th}}$ rotational state:

$$CO_2(0,0,1;19) + h\nu \rightarrow CO_2(1,0,0;20) + 2h\nu. \qquad (3.2.4.1)$$
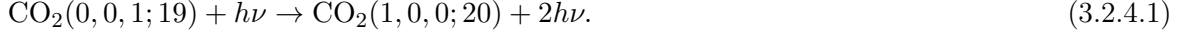
In section 2.1.3 we calculated the change in energy density in a two level system due to some spectral density ρ_ν. In this model, ρ_ν are all photons of frequency ν. So we use $\rho_\nu = E_\nu$. We thus have:

$$\frac{\partial E_\nu}{\partial t} = h\nu \left[\frac{N_{\text{up}}}{\tau_{\text{sp}}} + W\Delta N \right],$$

with

$$W = A_{21} \frac{c^3}{8\pi h\nu^3} g(\nu - \nu_0), \qquad (3.2.4.2)$$

$$\Delta N = \left(N_{\text{up}} - \frac{g_2}{g_1} N_{\text{lo}} \right). \qquad (3.2.4.3)$$

To calculate N_{up} and N_{lo} we need to find the population of the upper laser level (N_3), and the lower laser level (N_1). Then we need to find the fraction of those populations that are in the 19$^{\text{th}}$ and 20$^{\text{th}}$ rotational level respectively.

To find N_1 and N_3 we make use of the vibrational partition function, which results in [6, ch. 2.6]:

$$N_\lambda = N_{CO_2} \exp\left(\frac{h\nu_\lambda}{kT_\lambda} \right) \left[1 - \exp\left(\frac{h\nu_1}{kT_1} \right) \right] \left[1 - \exp\left(\frac{h\nu_2}{kT_2} \right) \right]^2 \left[1 - \exp\left(\frac{h\nu_3}{kT_3} \right) \right], \qquad (3.2.4.4)$$

with $\lambda = \{1, 3\}$.

To then find the fraction of molecules that are in the jth rotational level we use the rotational partition function, resulting in:

$$P(j) = \frac{2hcB}{kT}(2j + 1) \exp\left[\frac{hcBj(j+1)}{kT} \right], \qquad (3.2.4.5)$$

where B is the moment of inertia of the CO_2-molecule as defined in 3.1.1.4.

Thus we find:

$$N_{\text{up}} = N_3 P(19) \qquad (3.2.4.6)$$
$$N_{\text{lo}} = N_1 P(20) \qquad (3.2.4.7)$$

The linewidth of the laser is dependent on the pressure of the gas. For low pressures, Doppler shifts of the transition frequencies will be the main cause of line broadening. At higher pressures, the influence of collisional processes becomes much more prominent. According to [2, ch. 3.4] this results in:

$$g(\nu - \nu_0) \quad = \quad \frac{2}{2\pi\Delta\nu} \tag{3.2.4.8}$$

$$\Delta\nu \quad = \quad p_0 \cdot 7.58 \left(f_{CO_2} + 0.73 f_{N_2} + 0.64 f_{He}\right) \sqrt{\frac{300}{T}} \cdot 10^6 \tag{3.2.4.9}$$

where p_0 is the pressure of the gas in [Torr], and f_i is the fraction of the respective gases in the mixture. The other factors were determined experimentally.

3.2.4.1 Laser output

As the light travels back and forth through the laser, each round trip a fraction of the light is lost due to e.g. light that is not reflected back into the cavity, losses within the glass, mirrors, etc. Each process m that causes loss of energy can be quantified using a characteristic time constant τ_m, with [1, 4]:

$$\frac{1}{\tau_m} = -\frac{c}{2l_r} \ln[1 - \mathcal{L}_m], \tag{3.2.4.10}$$

where l_r is the length of the resonator and $\mathcal{L}_m$ is the fractional loss of energy per round trip.

The total change in energy due to losses is then given by:

$$\left.\frac{\partial E_\nu}{\partial t}\right|_{loss} = -\frac{E_\nu}{\tau_u}, \tag{3.2.4.11}$$

where

$$\frac{1}{\tau_u} = \sum_m \frac{1}{\tau_m}. \tag{3.2.4.12}$$

One of the mirrors of the laser is only partially reflective. This means that the output power of the laser can be determined by

$$P_{out} = \left.\frac{\partial E_\nu}{\partial t}\right|_{out} V_{am} = -\frac{E_\nu}{\tau_{out}} V_{am}, \tag{3.2.4.13}$$

where V_{am} is the volume of the active medium, and

$$\frac{1}{\tau_{out}} = -\frac{c}{2l_r} \ln[1 - \mathcal{T}], \tag{3.2.4.14}$$

with $\mathcal{T} = 0.4$ the transmission coefficient of the mirror.

3.2.4.2 Influence of lasing on the energy reservoirs

As the lasing process occurs, CO_2-molecules go from the asymmetric stretch mode to the symmetric stretch mode. This means that the energy in their respective reservoirs changes by the net number of molecules that change state multiplied by the energy of the level:

$$\frac{\partial E_3}{\partial t}\bigg|_{\text{laser}} = -G_3 \left[\frac{N_{\text{up}}}{\tau_{\text{sp}}} + W\Delta N\right] \tag{3.2.4.15}$$

$$\frac{\partial E_1}{\partial t}\bigg|_{\text{laser}} = +G_1 \left[\frac{N_{\text{up}}}{\tau_{\text{sp}}} + W\Delta N\right] \tag{3.2.4.16}$$

Also, the rotational quantum number changes from 19 to 20, this must be accounted for in E_{TR}:

$$\frac{\partial E_{\text{TR}}}{\partial t} = +(e_{\text{R}}(20) - e_{\text{R}}(19)) \left[\frac{N_{\text{up}}}{\tau_{\text{sp}}} + W\Delta N\right], \tag{3.2.4.17}$$

with $e_{\text{R}}(j)$ as defined in equation 3.1.1.2.

Through spontaneous emission photons are emitted in any direction. However, in E_ν only photons that travel in the direction of the laser are accounted for, other photons do not contribute. Therefore a factor ϕ is introduced, representing the angle within which photons do contribute to the reservoir:

$$\phi = 1 - \cos(\alpha), \tag{3.2.4.18}$$

$$\tan(\alpha) = \frac{r_{\text{d}}}{2l_{\text{r}}}, \tag{3.2.4.19}$$

where r_{d} is the radius of the discharge and l_{r} is the length of the resonator.

This finally gives us

$$\frac{\partial E_\nu}{\partial t}\bigg|_{\text{laser}} = -\frac{E_\nu}{\tau_{\text{u}}} + h\nu \left[\phi\frac{N_{\text{up}}}{\tau_{\text{sp}}} + W\Delta N\right] \tag{3.2.4.20}$$

3.3   Complete model

By combining the equations for each energy reservoir, we find the complete system of differential equations. The terms in each equation are sorted by the processes as described above: pumping, V-T and V-V collisions, gas cooling and photon processes. Figure 3.2 shows the reservoirs E_1, E_2, E_3, and E_4, and the processes between them.

$$
\begin{aligned}
\frac{\partial E_{\mathrm{TR}}}{\partial t} = \\
&+ \left(\chi_{\mathrm{T}} + \chi_{\mathrm{R}} \right) P_{\mathrm{in}} \\
&+ \frac{E_1 - E_1^{\mathrm{eq}}(T)}{\tau_{10}} + \frac{E_2 - E_2^{\mathrm{eq}}(T)}{\tau_{20}} + \frac{E_4 - E_4^{\mathrm{eq}}(T)}{\tau_{40}} \\
&+ \left(1 - \frac{G_1}{G_3} - \frac{G_2}{G_3} \right) \frac{E_3 - E_3(T, T_1, T_2)}{\tau_3} + \left(1 - \frac{G_3}{G_4} \right) \frac{E_4 - E_4(T)}{\tau_{43}} \\
&- \frac{E_{\mathrm{TR}} - E_{\mathrm{TR}}(T_0)}{\tau_{\mathrm{d}}} \\
&+ \left(e_{\mathrm{R}}(20) - e_{\mathrm{R}}(19) \right) \left[\frac{N_{\mathrm{up}}}{\tau_{\mathrm{sp}}} + W \Delta N \right]
\end{aligned}
\tag{3.3.0.1}
$$

$$
\begin{aligned}
\frac{\partial E_1}{\partial t} = \\
&+ \chi_1 P_{\mathrm{in}} \\
&- \frac{E_1 - E_1^{\mathrm{eq}}(T)}{\tau_{10}} \\
&- \frac{E_1 - E_1(T_2)}{\tau_{12}} + \frac{G_1}{G_3} \frac{E_3 - E_3(T, T_1, T_2)}{\tau_3} \\
&- \frac{E_1 - E_1(T_0)}{\tau_{\mathrm{d}}} \\
&+ G_1 \left[\frac{N_{\mathrm{up}}}{\tau_{\mathrm{sp}}} + W \Delta N \right]
\end{aligned}
\tag{3.3.0.2}
$$

$$
\begin{aligned}
\frac{\partial E_2}{\partial t} = \\
&+ \chi_2 P_{\mathrm{in}} \\
&- \frac{E_2 - E_2^{\mathrm{eq}}(T)}{\tau_{20}} \\
&+ \frac{E_1 - E_1(T_2)}{\tau_{12}} + \frac{G_2}{G_3} \frac{E_3 - E_3(T, T_1, T_2)}{\tau_3} \\
&- \frac{E_2 - E_2(T_0)}{\tau_{\mathrm{d}}}
\end{aligned}
\tag{3.3.0.3}
$$

$$\frac{\partial E_3}{\partial t} =$$
$$+ \chi_3 P_{\text{in}}$$
$$- \frac{E_3 - E_3(T, T_1, T_2)}{\tau_3} + \frac{G_3}{G_4} \frac{E_4 - E_4(T_4)}{\tau_{43}}$$
$$- \frac{E_3 - E_3(T_0)}{\tau_{\text{d}}}$$
$$- G_3 \left[\frac{N_{\text{up}}}{\tau_{\text{sp}}} + W \Delta N \right]$$

$$(3.3.0.4)$$

$$\frac{\partial E_4}{\partial t} =$$
$$+ \chi_4 P_{\text{in}}$$
$$- \frac{E_4 - E_4^{\text{eq}}(T)}{\tau_{40}}$$
$$- \frac{E_4 - E_4(T_4)}{\tau_{43}}$$
$$- \frac{E_4 - E_4(T_0)}{\tau_{\text{d}}}$$

$$(3.3.0.5)$$

$$\frac{\partial E_\nu}{\partial t} =$$
$$- \frac{E_\nu}{\tau_{\text{u}}} + h\nu \left[\phi \frac{N_{\text{up}}}{\tau_{\text{sp}}} + W \Delta N \right]$$

$$(3.3.0.6)$$
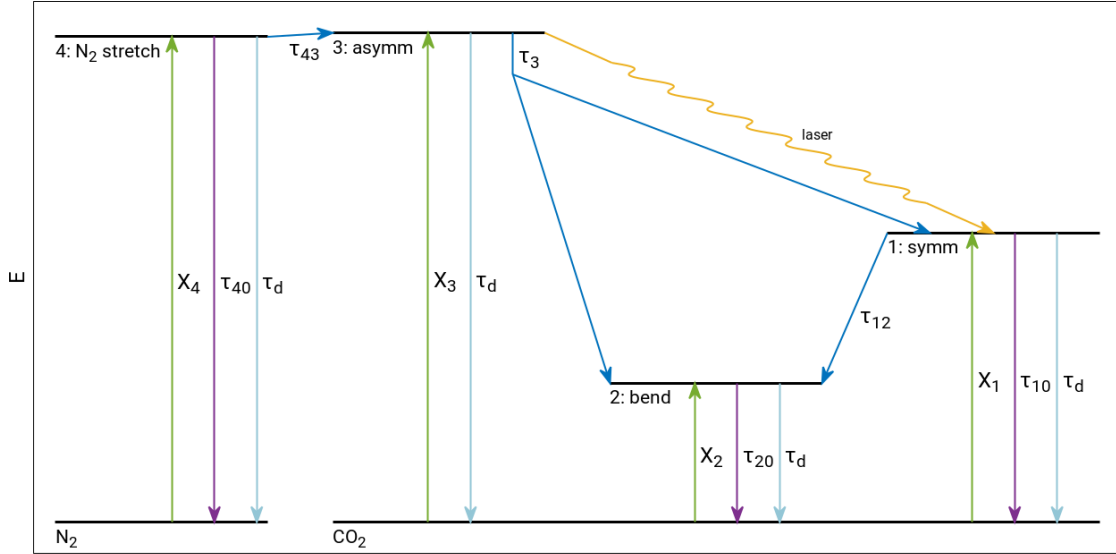
Figure 3.2: A representation of the energy levels of the excited states of N_2 and CO_2, and included processes in the five temperature model: pumping in green, V-V interactions in dark blue, V-T interactions in purple, and cooling in blue. The laser transition is the wavy line in yellow. The pumping fractions and decay rates for the respective processes are included.

3.4 Energy conservation

By summing the system of differential equations: $\frac{\partial E}{\partial t} = \frac{\partial}{\partial t}(E_{\text{TR}} + E_1 + E_2 + E_3 + E_4 + E_\nu)$, we find an equation that describes the total power entering or leaving the system at any time:

$$\frac{\partial E}{\partial t} = (1 - \chi_{\text{el}}) P_{\text{in}} - \sum_i \frac{E_i - E_i^{T_0}}{\tau_d} - \frac{E_\nu}{\tau_{\text{u}}} - h\nu(1 - \phi)\frac{N_{\text{up}}}{\tau_{\text{sp}}}. \tag{3.4.0.1}$$

This is a useful tool to check whether the numerical solution matches the analytical result.

Chapter 4

Results and Discussion

This chapter will discuss the results found using our implementation of the five temperature model. First we will discuss the parameters and solvers used in all of the simulations, unless noted otherwise. Using those parameters we determined what relative tolerance setting was necessary to find consistent results. Then we ran the simulation in both MATLAB and PLASIMO, so we could verify the results of our implementation. Using equation 3.4.0.1 the conservation of energy in the simulation was checked.

In MATLAB, changing the input parameters would sometimes cause the simulation to crash. To test the robustness of the implementation in PLASIMO, simulations were ran using the default parameters, changing one at a time. These parameter studies show that the PLASIMO implementation is very reliable.

To validate the results of the model, some simulations were done and compared to other results in literature. Also, some simulations of real world applications of a CO_2 laser were done.

4.1 Program

4.1.1 Simulation parameters

Table 4.1 shows an overview of the parameters that were used in all simulations, unless noted otherwise.

parameter	symbol	value	unit
pressure	p_0	$130 \cdot 10^2$	Pa
temperature	T_0	300	K
input power	P_{in}	$1.706794 \cdot 10^7$	W/m^3
	χ_{TR}	0.01436	
	χ_1	0.01591135	
pumping fractions	χ_2	0.01591135	
	χ_3	0.03649	
	χ_4	0.85301	
	f_{CO_2}	0.03	
mixture fractions	f_{N_2}	0.77	
	f_{He}	0.20	

Table 4.1: An overview of the parameters used in all simulations, unless noted otherwise.

Since the model calculates an energy density, we also need to know the volume of the active medium to find the output power of the laser. The radius of a discharge is 1.2 cm, and its length is 30 cm. There are 8 discharges in total, making the volume $V \approx 1.09 \cdot 10^{-3}$ m^3.

4.1.2 Solvers used

The results of the models in MATLAB and PLASIMO are very similar, though there are some differences. Of course the initial conditions in each simulation must be exactly the same, and they are. Differences in the results are caused by each program using a different solver: MATLAB uses ode45 [10], whereas in PLASIMO the LSODA solver from ODEPACK is used [11].

4.2   Determining acceptable tolerances

While some problems can be solved quickly and accurately using a high tolerance, other, stiffer problems may require a much lower tolerance to get good results. Our problem is quite stiff: some processes, such as the change of the inversion population when the laser starts up, require very small time steps to be simulated accurately. However, compared to the start up, it takes a long time before the system stabilizes, thus requiring many steps. The solvers used in PLASIMO can adjust the size of the time step, so fast processes are calculated accurately, while simultaneously preventing long simulation times.

As such, it is also important to find the right relative tolerance setting. Too high, and the results will be inaccurate. Too low, and the simulation will take much longer than is necessary.

In MATLAB, the relative tolerance of the solver is set to 10^{-7}. To investigate which relative tolerance is acceptable for usage in PLASIMO, the results of simulations at various values were compared to the results of MATLAB. One characteristic feature of the photon energy density is especially useful for comparing results. Once population inversion has been reached, a sharp peak will occur in the photon energy density. The time at which this effect occurs depends on the tolerance chosen. The difference is very small though; see figure 4.1.

The results, although very similar, differ slightly depending on the tolerance. The difference between simulations at relative tolerances of 10^{-9} and 10^{-12} in PLASIMO is barely visible. Since even at very small tolerances the computation time is only a few seconds, a tolerance of 10^{-12} was chosen for all other simulations.

To demonstrate the effect of incorrectly chosen tolerances, the results of a simulation in PLASIMO at a relative tolerance of 10^{-5} is included. Although the steady state solution is the same as in the other simulations, when there is a lot of change in the system the result is very inaccurate.
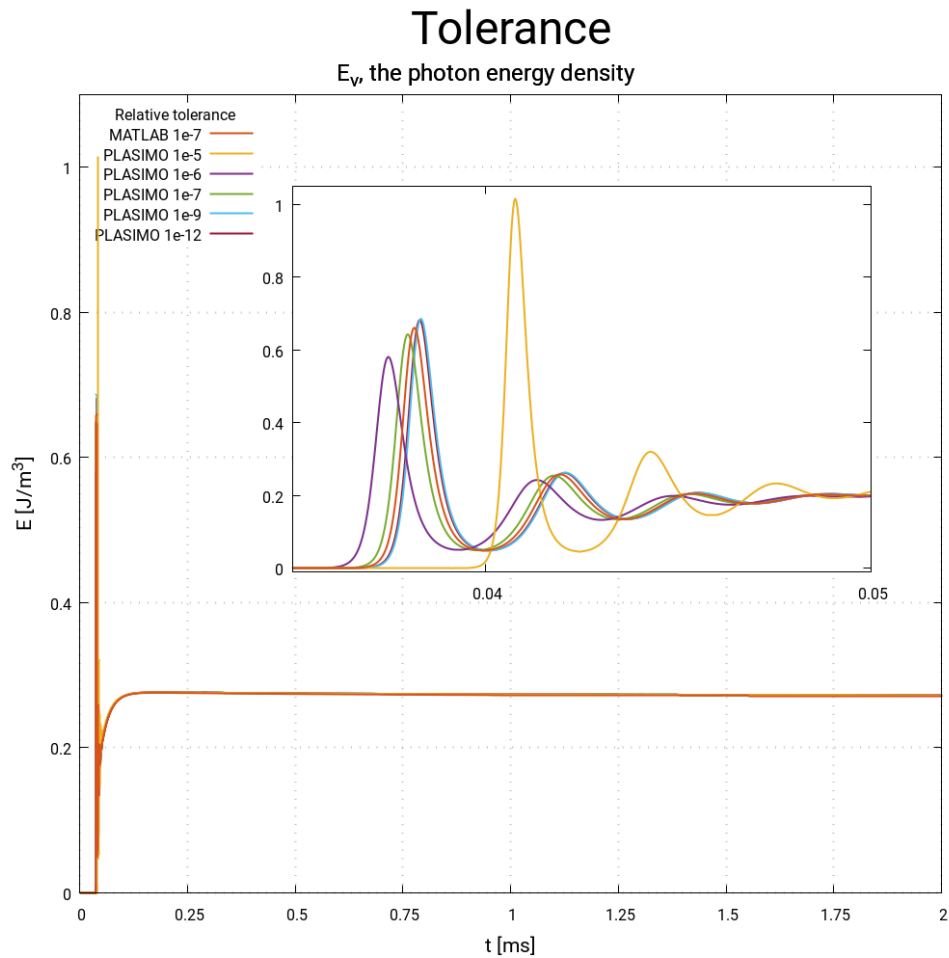
Figure 4.1: E_ν for several different settings of relative tolerances in PLASIMO, compared to the result of MATLAB. The difference between the results of simulations at tolerances of of 10^{-9} and 10^{-12} is barely visible, even in the insert showing a close up.

4.3 Verification

4.3.1 Output of the model at default parameters

The model has a lot of outputs: energy densities, temperatures, relaxation times. For completeness, all results from a simulation using the standard input parameters were included in this section.

4.3.1.1 The energy densities

Figure 4.2 shows the behaviour of the energy reservoirs during the simulation. When population inversion is reached, the gas heats up tremendously.

A closer look at the reservoirs E_1, E_2, E_3 and E_4 is shown in 4.3. From the start, E_4 increases greatly because of the pumping. As the N_2 is excited, energy is transfered to E_3 through V-V collisions. Meanwhile, E_2 barely gains any energy. As soon as population inversion is reached, we can see a sharp decrease in energy of E_3, while at the same time that of E_2 increases. The loss in energy of E_3 is quickly compensated for by E_4, whose energy slowly stabilizes. Most energy goes to E_{TR} as the gas is heated up through V-T interactions.

4.3.1.2 The 5 temperatures

See figure 4.4. As soon as the laser is turned on, T_4 increases very quickly, and because of the V-V interactions between N_2 and CO_2 T_3 increases as well.

As soon as population inversion is reached a lot happens. T_3 and T_4 still increase, but much slower than before. T_1 and T_2 show a sharp increase. Since the lower laser level is being drained through a V-T interaction with He, the gas temperature immediately increases as well. All temperatures stabilize over time, as the gas in the laser is being refreshed. However, this takes longer than the 2 ms duration of the simulations.

The results from MATLAB and PLASIMO agree very well, although there are some minor differences in the end.

4.3.1.3 The relaxation times

The relaxation times are compared in figure 4.5, using a logarithmic scale since the orders of magnitude of the processes are vastly different.

Although these relaxation times barely change during the simulation, there still are a few interesting observations to be made. First, τ_{40} is much higher than τ_{43}. This means that excited N_2 molecules can much easier transfer their energy to CO_2 than through other means. This is what makes N_2 such an excellent species for excitation of CO_2.

The second highest relaxation time is that of the upper laser level: τ_3. This means that CO_2 molecules in the asymmetrical stretch mode are relatively long lived.

The depopulation of the lower laser level goes through two paths. Direct V-T transitions to the ground state are described by τ_{10}, which already is about 10 times lower than τ_3. However, this pales in comparison to V-V interactions where molecules transition to the bending mode: τ_{12} is approximately 1000 times smaller than τ_{10}. In turn, the bending mode relaxes to the ground state through V-T interactions, described by τ_{20}.

Because of this combination of relaxation times, population inversion can be achieved.

The results for MATLAB and PLASIMO are almost exactly the same. Since the relaxation times only change very little throughout the simulation, we will pay them no further mind in the rest of the results.

Figures 4.2, 4.3, 4.4 and 4.5 give a good indication of the order of magnitude of the energy densities, temperatures and relaxation times, and show that the results from MATLAB and PLASIMO are very similar. However, to better compare individual energy densities or temperatures, we will take a closer look at them in some of the next simulations.
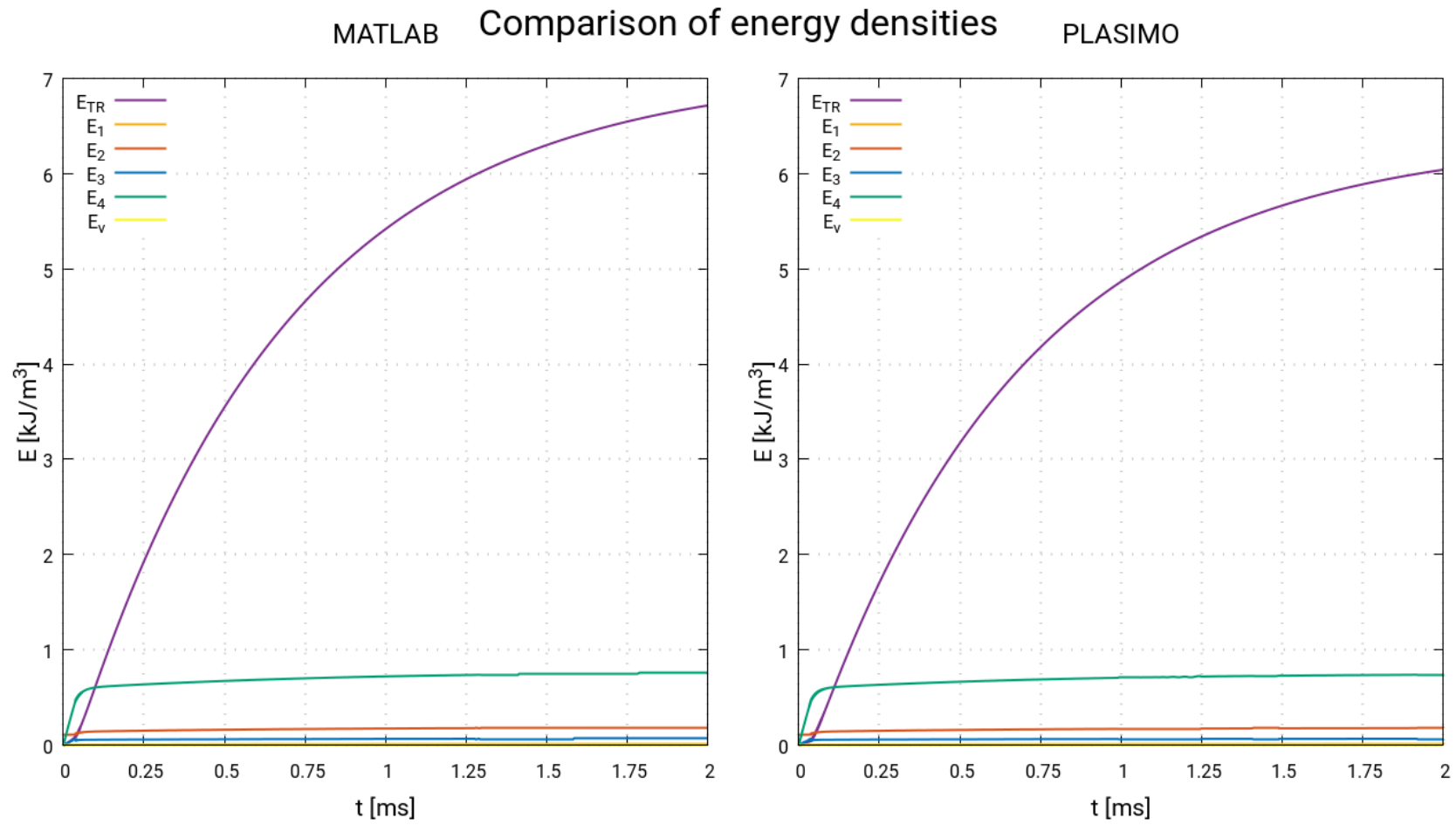
Figure 4.2: The results of the energy density of simulations in MATLAB and PLASIMO using the same input parameters.
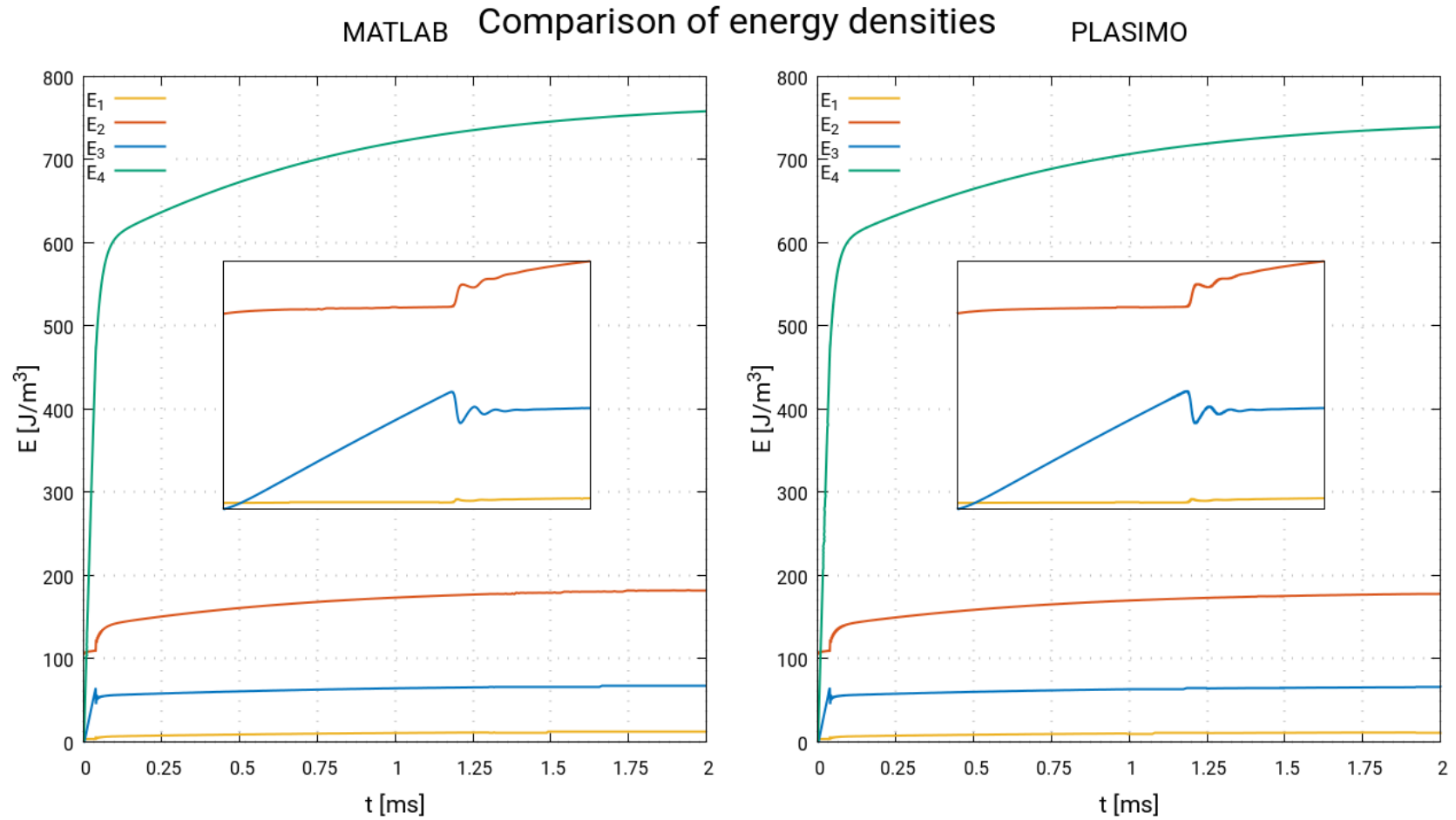
Figure 4.3: The results of the vibrational energy density reservoirs of simulations in MATLAB and PLASIMO using the same input parameters. The insert shows the effect of reaching population inversion on the E_1, E_2 and E_3.
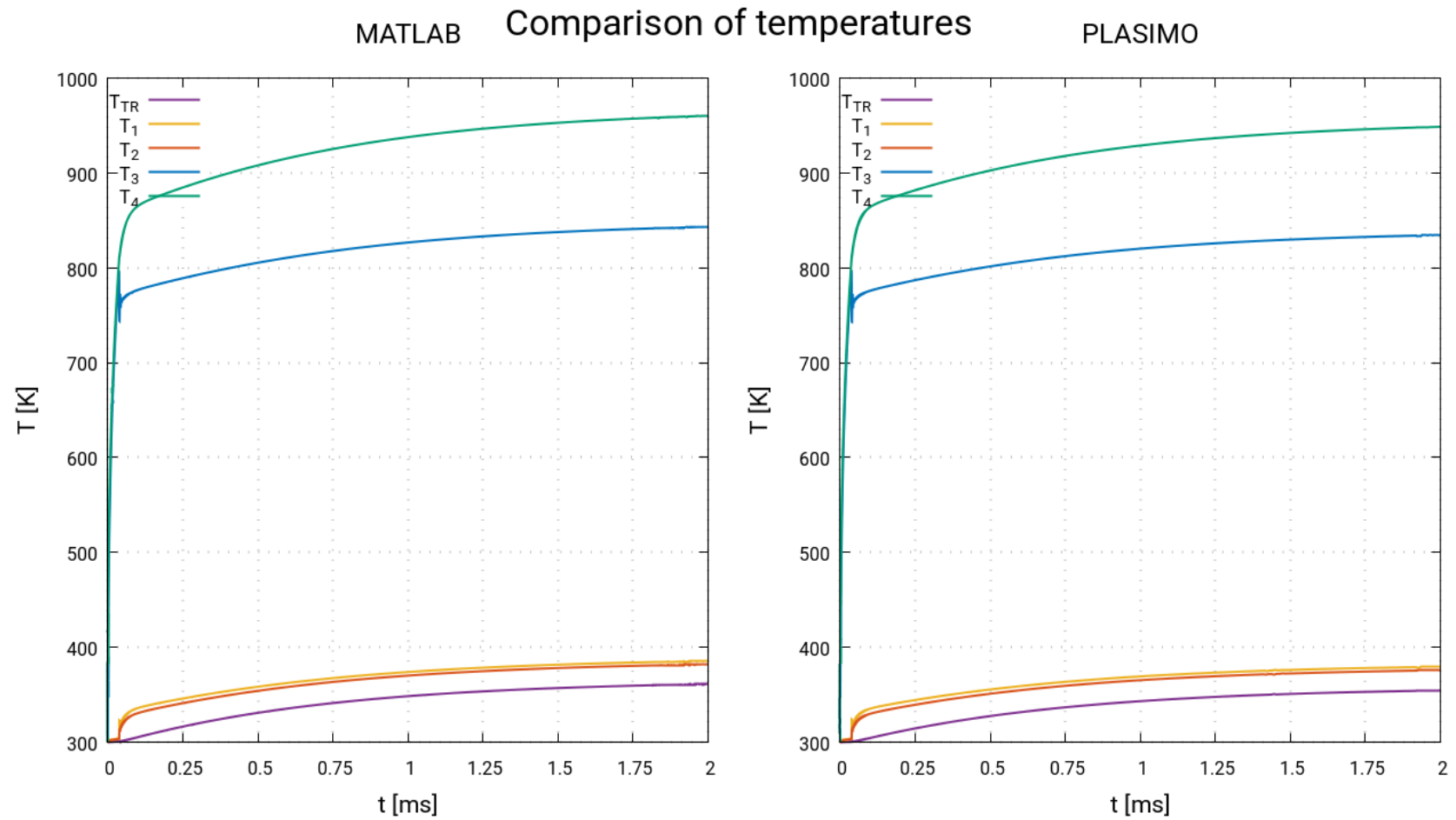
Figure 4.4: The results of simulations in MATLAB and PLASIMO using the same input parameters. When population inversion is reached, the effect is clearly noticeable on all vibrational temperatures, as well as the gas temperature.
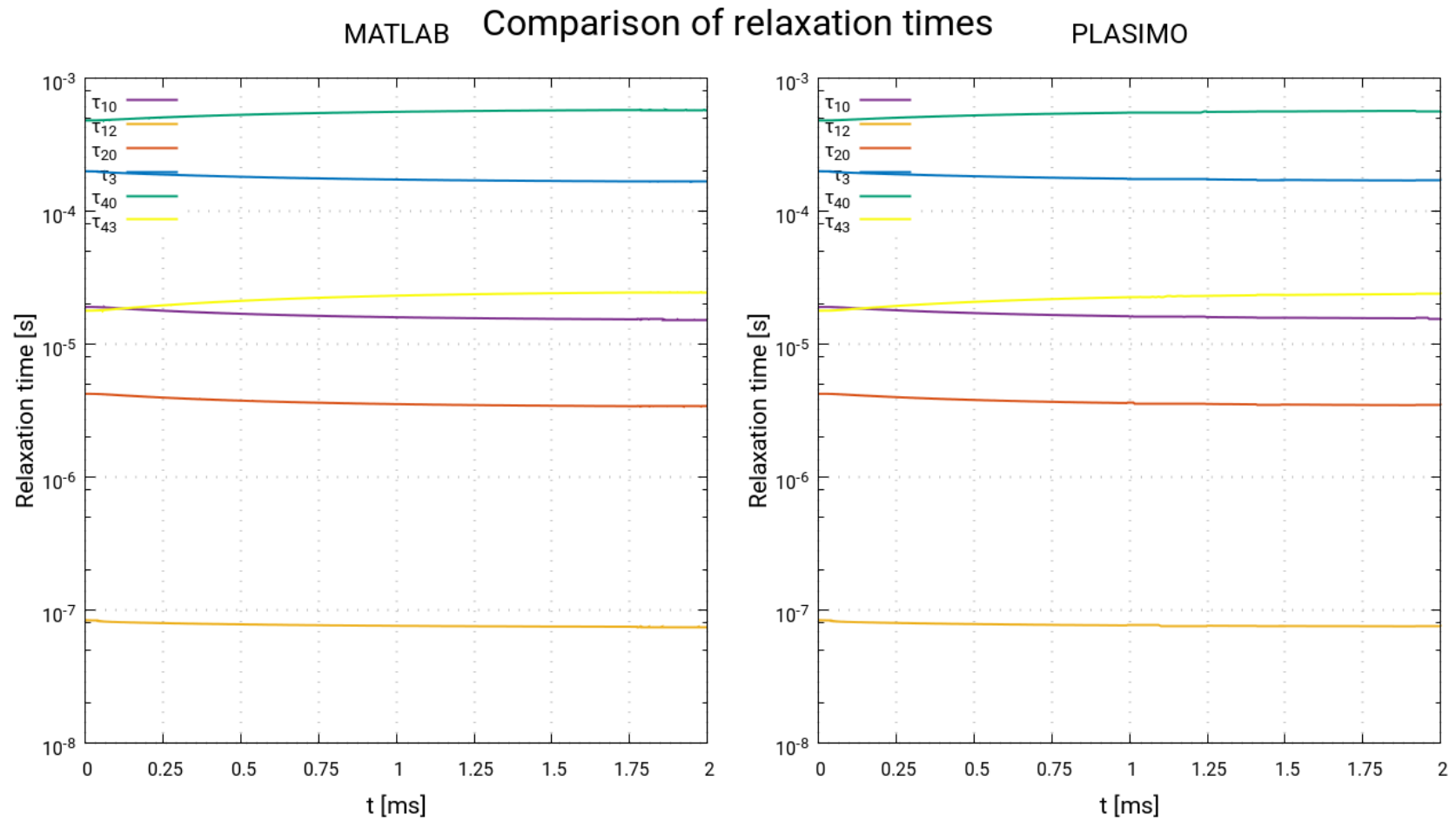
Figure 4.5: The results of simulations in MATLAB and PLASIMO using the same input parameters, plotted on a logarithmic scale. Although the relaxation times don't change much, they tell a lot about the speed at which the processes occur.

4.4 Checking the energy balance

Using equation 3.4.0.1, a check was made to ensure that the numerical solution matched the analytical result. An error was discovered in the application of the pumping terms χ_i. This was clearly visible because when the power was turned on, there would be a difference between the change in energy that was theoretically expected, and the value that was calculated numerically. When the power was turned off, this difference would disappear. This can be seen in image 4.6. A rounded pulse was used for the input power, to clearly show the effect.

For all other results shown in this report, including the previous ones, this error was corrected.
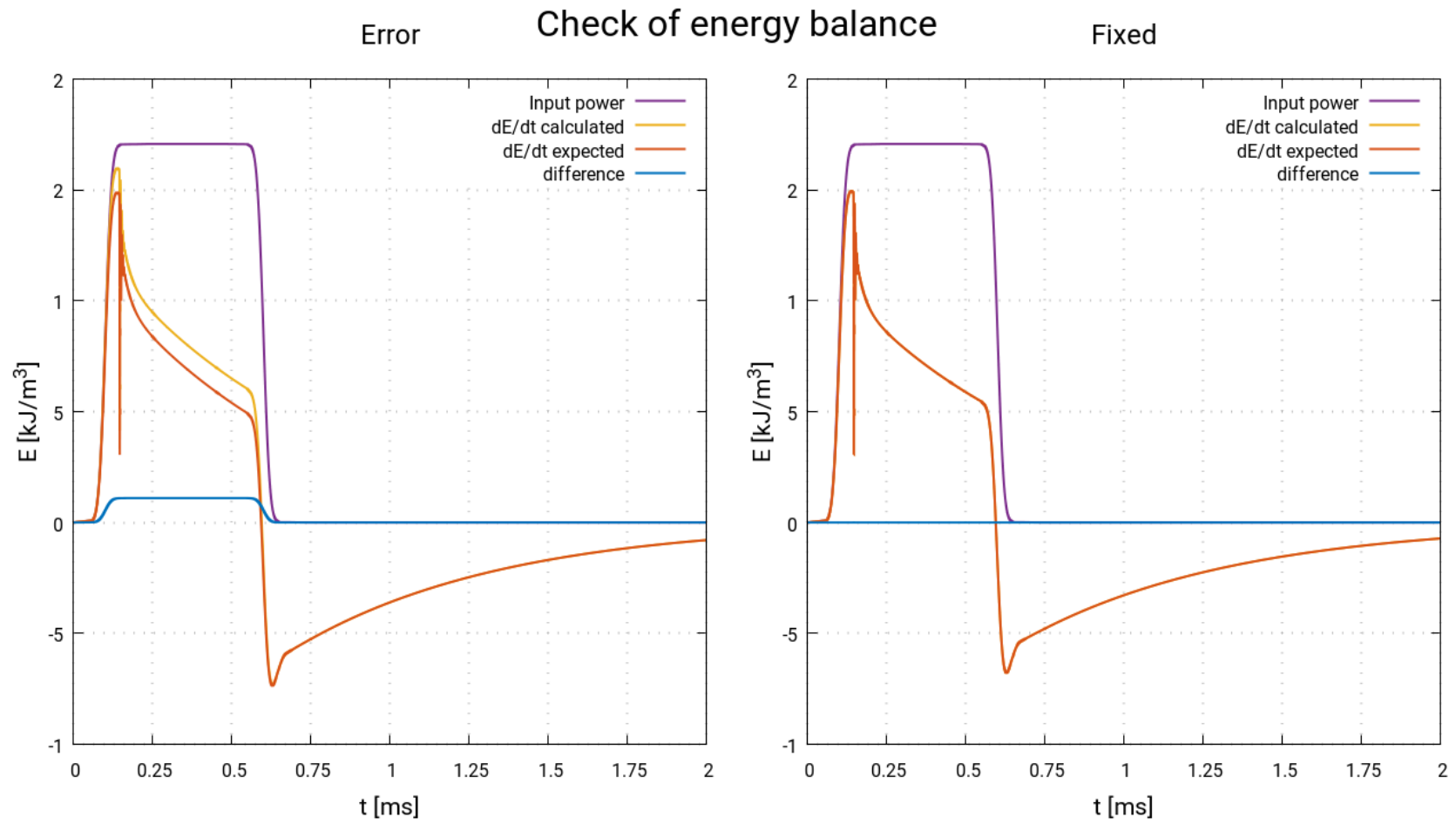
Figure 4.6: An error was found and corrected in the energy balance of the model.

4.5 Parameter studies

When changing the input parameters, sometimes the MATLAB program has trouble finding a solution. To test which parameters caused the problems, various inputs were tested in MATLAB. The same input was then given to PLASIMO, to test whether it was able to solve the problems that MATLAB could not. Note that these results do not represent realistic cases. In reality, the pumping terms depend on other parameters, such as pressure and input power. In order to get comparable results, only one parameter was changed at a time, keeping the others constant.

4.5.1 Varying the pumping terms

For testing purposes, the pumping terms were kept constant in all simulations. However, in practice, these values will be generated by BOLSIG+, a solver of the Boltzmann equation. It is therefore important that the model be able to generate a solution regardless of the input values. The values were varied in such a way that the lower laser level would be populated far more than in the standard test case, and the upper laser level and the pumping gas would gain much less energy. Both MATLAB and PLASIMO were able to calculate solutions for each set of parameters without issue.

4.5.2 Varying the pressure

Simulations were done for various pressures, ranging from one half of the default pressure up to four times as high. In the simulation where the pressure was 52000 Pa, the population of the lower laser level was too high, and population inversion was never reached. This can be seen very well in the results of E_3 in Figure 4.7. The results from MATLAB and PLASIMO only slightly differ from each other; even in the close up views the difference is barely visible. The steady state solution does show some slight difference.
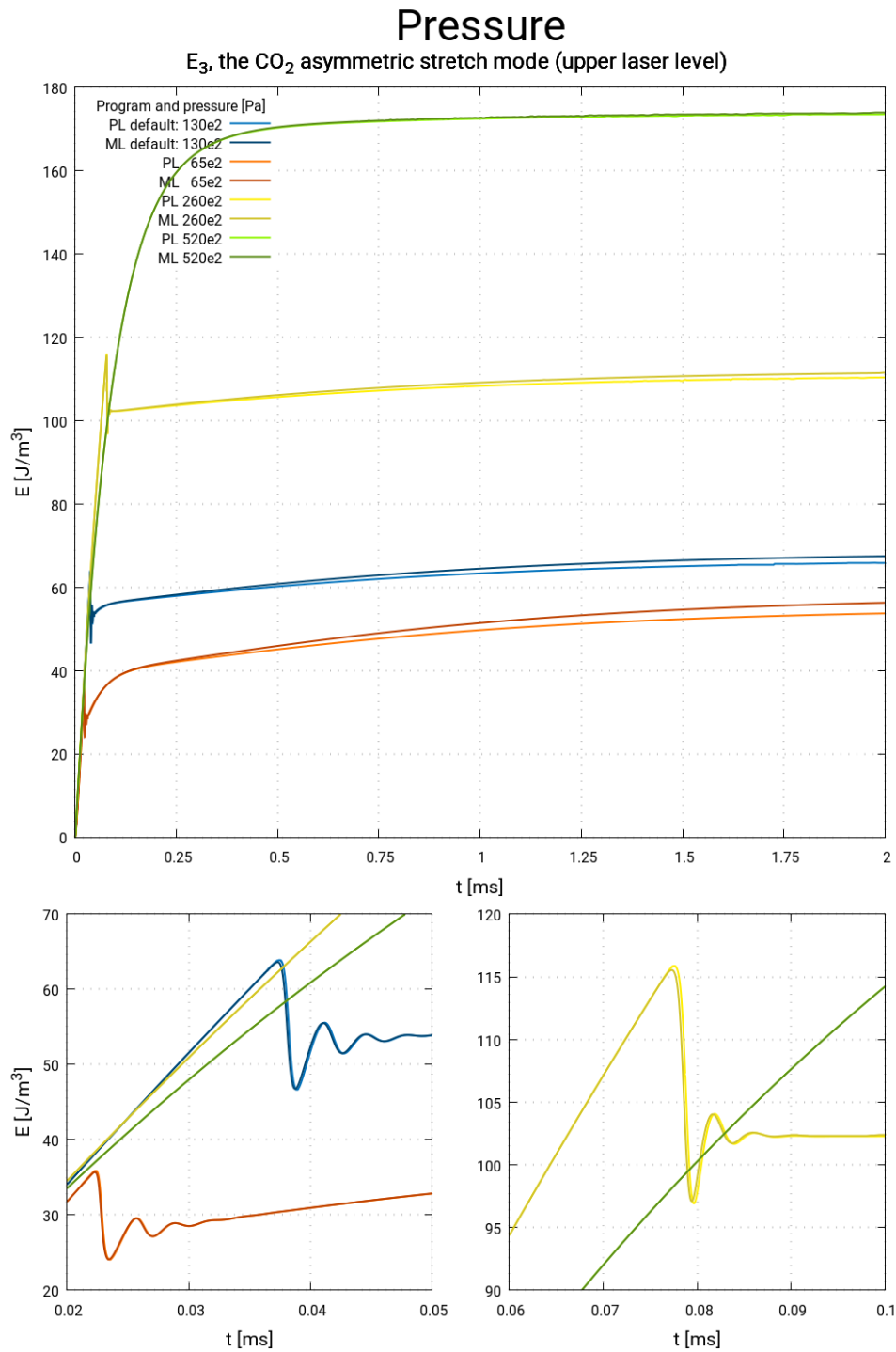
Figure 4.7: Results of simulations in MATLAB and PLASIMO for various pressures.

4.5.3 Varying the input power

The total input power was varied from 0.5 times up to 10 times the default input power. At 10 times the usual input power proved to be a very challenging problem for MATLAB's solvers: after simulating about 1.1 ms, the solver started giving the following message: "Warning: Matrix is close to singular or badly scaled. Results may be inaccurate." In figure 4.8 this can be clearly seen, where a sharp peak occurs in E_3.

Whereas other simulations usually took no longer than a few minutes in MATLAB, this one took over 15 hours to complete. In PLASIMO the simulation was completed in a few seconds.
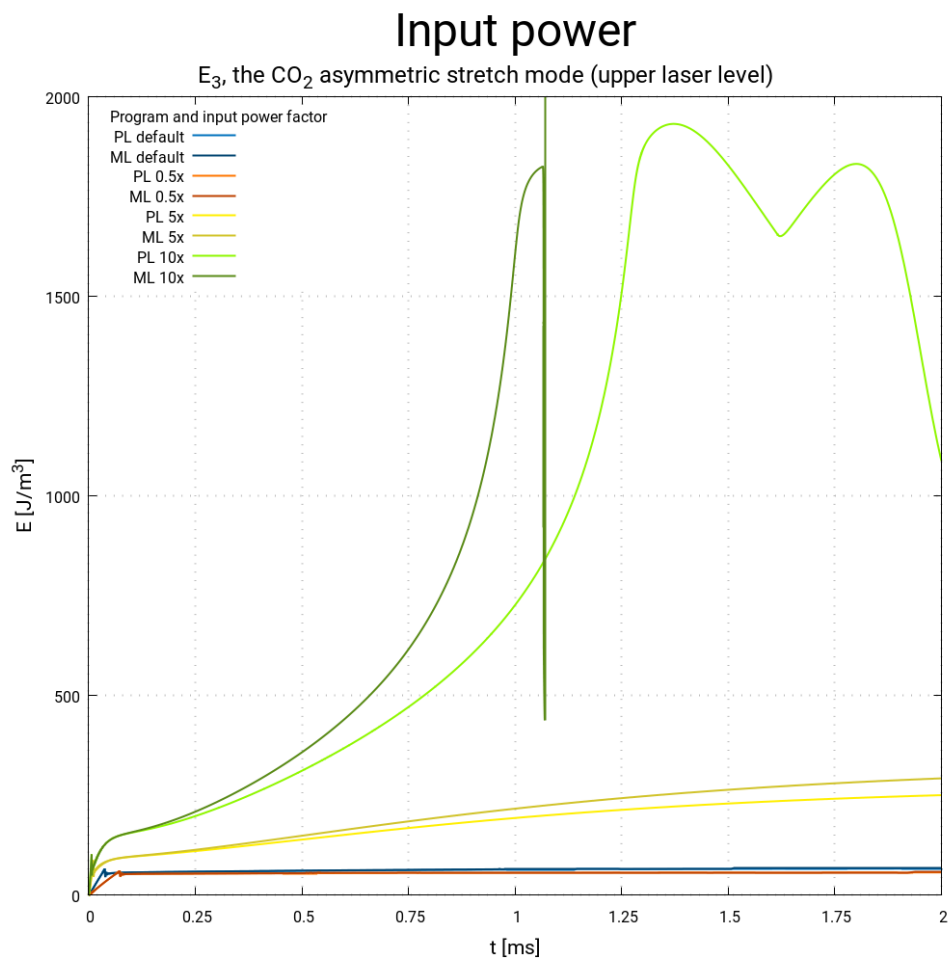
Figure 4.8: Results of simulations in MATLAB and PLASIMO for various input power settings. At very high input powers, the system becomes unstable as the gas heats up too much.

4.6   Simulations of real world applications

Many lasers are operated by regulating the input power to achieve some desired effect. As a proof of concept, some variations were tested that have real world applications.

The model is validated through the realistic results of these simulations.

4.6.1   Pulsed input power

There are many cases in which the laser may need to be turned on and off again quickly, such as when etching an image, or for welding objects that must not become too hot.

To simulate this, the input power was pulsed at a duty cycle of 50% for frequencies of 1 up to 10 kHz. Figure 4.9 shows the output power of some of the results. When the power is turned on, it takes a while before the laser actually produces light. When it is turned off, there is still energy left in the reservoirs and the output of the laser slowly decays. As the frequency becomes higher, the upper and lower laser level cannot lose all of their energy before being pumped again. As a result, the initial peak is much smaller. However, at those frequencies the laser never really stops emitting light. For certain sensitive applications even if the laser only emits 10^{-3} of the steady state output of light, that could still be too much.

These results agree very well with results found in literature [4, fig. 2.2.5.g4].

4.6.2   Rounded pulse

In reality a square input pulse will never be perfectly square. A simulation was run where the input was shaped like a rounded square pulse. The pulse shape was calculated using a damped Fourier series [4, ch 2.2.2]:

$$
P_{\text{in}}(t) \;=\; \frac{A_0}{2}\frac{T_1}{T/2} \tag{4.6.2.1}
$$

$$
+ \sum_{m=1}^{\infty} \exp\left(-\gamma_m m\right) \frac{A_0}{m\pi} \left[\sin\left(\frac{m\pi T_1}{T/2}\right)\cos\left(\frac{m\pi t}{T/2}\right) + \left(1 - \cos\left(\frac{m\pi T_1}{T/2}\right)\sin\left(\frac{m\pi t}{T/2}\right)\right) \right],
$$

$$
\gamma_m \;=\; m \cdot 5 \cdot 10^{-3} \tag{4.6.2.2}
$$

The damping term $\exp\left(-\gamma_m m\right)$ was used to counteract Gibb's phenomenon. Because of this term, the normalization of the pulse is no longer A_0. Therefore, the pulse was translated so that the minimal input power was 0, and then scaled so that the maximum was A_0.

This pulse shape also serves as a proof of concept to show that the input power can be in whatever shape is desired.

In fig 4.6 this pulse shape was used to validate the energy balance.

4.6.3 Slow start

When the input power is turned on fully, there will be a large peak in the output power when the laser threshold is reached. This can be an undesirable effect, e.g. when a laser is used for etching and the output must remain below a certain maximum so that it does not burn a hole in the sample. In that case a so called *slow start* can be used. The input power is slowly raised from 0 to the maximum. This way, when the threshold is reached, the population inversion is smaller and the peak power will be much lower.

As shown in figure 4.10, the start up peak of the laser is already lower than the maximum laser output, when using a start up time of only 0.5 ms.
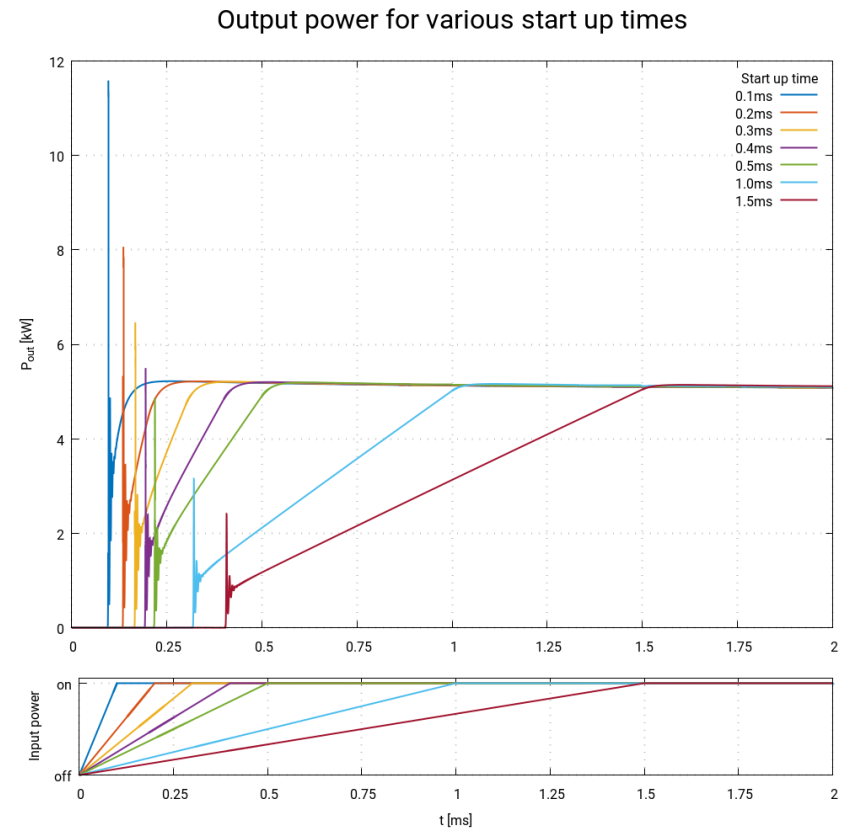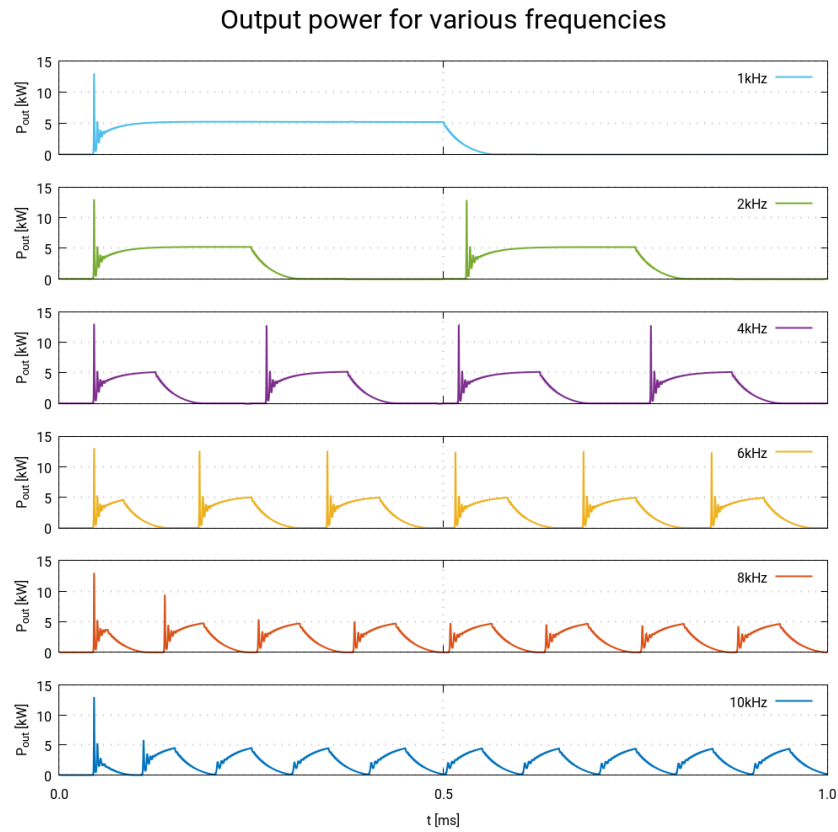
Figure 4.9: The output power of the laser when the input is pulsed at a duty cycle of 50% at frequencies from 1kHz up to 10kHz. At high frequencies the start up peak almost disappears.

Figure 4.10: The output power for various start up times. For times longer than 0.5 ms the peak at the start is lower than the equilibrium value.

Chapter 5

Conclusion

Due to the many different applications of CO_2 lasers, a model that can simulate the output power of these lasers is desired. This model should be fast and reliable, for a broad range of input parameters. An existing implementation of the 5 temperature model in MATLAB is very slow, and in some cases fails to calculate a solution.

Therefore, the five temperature model was implemented in PLASIMO. An error in the code was found, and fixed, to ensure that energy within the system is conserved. The results of the PLASIMO implementation were successfully verified using the existing model in MATLAB. The robustness of the implementation was tested using a series of parameter studies. The program was able to calculate a solution for any given set of input parameters very quickly: a typical simulation is completed in just a few seconds.

To validate the model, results were compared to literature, showing the model gives very realistic results. Also, some simulations of real world applications were tested. This proves we can simulate input power shaped in any way desired, which used to be very difficult in the MATLAB implementation.

We can thus conclude that the model was successfully implemented in PLASIMO, and we now can reliably simulate the behaviour of a CO_2 laser, using any combination of input parameters as necessary.

Although the five temperature model already gives quite realistic results, there is plenty of room for improvements and additions. Some examples:

Pumping terms.
    In this model, the pumping term fractions χ_i are assumed to be constant. In reality, the collision cross sections depend on parameters such as pressure, electric field, etc. It is therefore important to choose correct parameters when running the model. An option would be to calculate or look up new values whenever these parameters change.

Amplifier model.
    The 5 temperature model would also be very suitable to use as a model for an amplifier. By discretizing space in the longitudinal direction, the amplification of an input pulse as it travels through the laser could be calculated.

Spatial effects.

Currently, spatial effects are not taken into account, the plasma is assumed to be equal at all points in space. This is de facto not the case; conditions in the sheath differ greatly from those in the center of the plasma. By dropping these simplifications, a profile of the laser output could be simulated.

Expanding the model.

The chemistry of the model could be expanded by adding more reservoirs and associated reactions, e.g. for CO. The laser transition between the asymmetric stretch mode and the bending mode could also be included, by adding another reservoir for photons of 9.6 μm.

Bibliography

[1] O. Svelto, *Principles of Lasers.* Springer New York Dordrecht Heidelberg London, 2010.

[2] W. Witteman, *The* CO_2 *laser.* Springer-Verlag Berlin Heidelberg GmbH, 1987.

[3] G. J. M. Hagelaar and L. C. Pitchford, "Solving the boltzmann equation to obtain electron transport coefficients and rate coefficients for fluid models," *Plasma Sources Sci. Technol.*, vol. 14, no. 4, pp. 722–733, 2005.

[4] D. Toebaert, *Experimenteel en Theoretisch Onderzoek naar de Vibrationele Kinetiek in het Plasma van een Axiaal Sneldoorstroomde* CO_2 *laser.* PhD thesis, Universiteit Gent, 1996.

[5] R. L. Abrams and P. K. Cheo, "Collisional relaxation of CO_2 rotational levels by N_2 and He," *Appl. Phys. Lett.*, vol. 15, no. 6, p. 177, 1969.

[6] K. Smith and T. R.M, *Computer Modeling of Gas Lasers.* New York: Plenum, 1978.

[7] K. R. Manes and H. J. Seguin, "Analysis of the CO_2 TEA laser," *Journal of Applied Physics*, vol. 43, no. 12, pp. 5073–5078, 1972.

[8] S. Sazhin, P. Wild, C. Leys, D. Toebaert, and E. Sazhina, "The three temperature model for the fast-axial-flow CO_2 laser," *J. Phys. D: Appl. Phys.*, vol. 26, no. 11, pp. 1872–1883, 1993.

[9] R. L. Taylor and S. Bitterman, "Survey of vibrational relaxation data for processes important in the $CO_2 - N_2$ laser system," *Reviews of Modern Physics*, vol. 41, no. 1, pp. 26–47, 1969.

[10] L. F. Shampine and M. W. Reichelt, "The matlab ode suite," *SIAM Journal on Scientific Computing*, vol. 18, pp. 1–22, 1997.

[11] A. C. Hindmarsh, *ODEPACK, A Systematized Collection of ODE Solvers*, vol. 1 of *IMACS Transactions on Scientific Computation.* R. S. Stepleman et al. (eds.), North-Holland, Amsterdam, 1983.